พระจอมเกล้าลาดกระบัง

Ionosphere and Equatorial Plasma Bubbles (EPB)

Jirapoom Budtho, Ph.D.

Telecommunications Engineering Department
Center of Excellence in GNSS & Space Weather
King Mongkut's Institute of Technology Ladkrabang (KMITL)
Email: jirapoom.bu@kmitl.ac.th

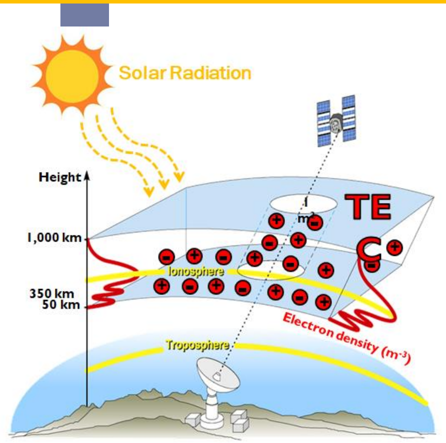

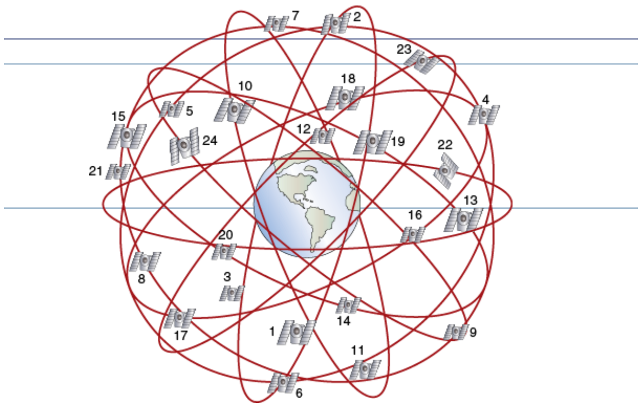

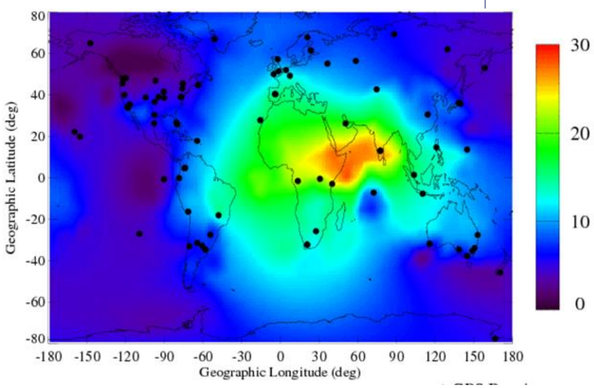

Types of EPB

- Post-sunset EPB
  - Solar max. periods
  - PRE dominates ESF process
  - More prevalent on equinocial months
- Post-midnight EPB
  - Solar min. periods especially solstice months
  - The role of gravity waves (GW) is evident
  - Occurrence rates increase with decrease of solar flux

Effects of EPB

Ionospheric delay gradient

Aeronautical navigation: Ground-based augmentation system (GBAS)

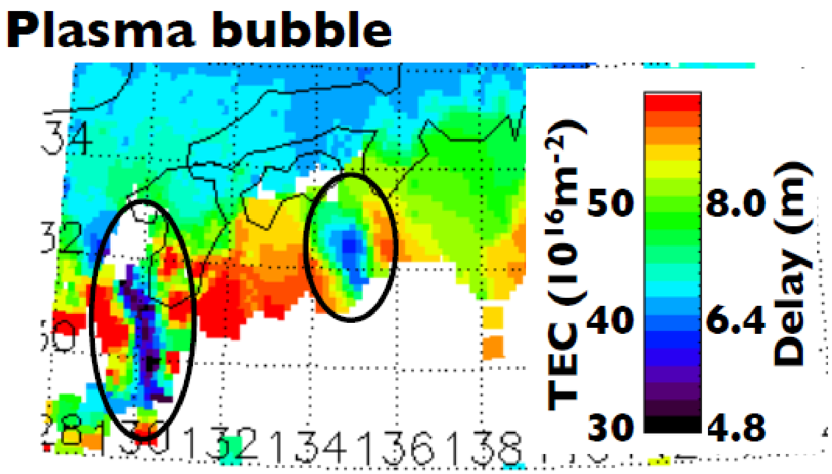

[S. Saito, 2011]

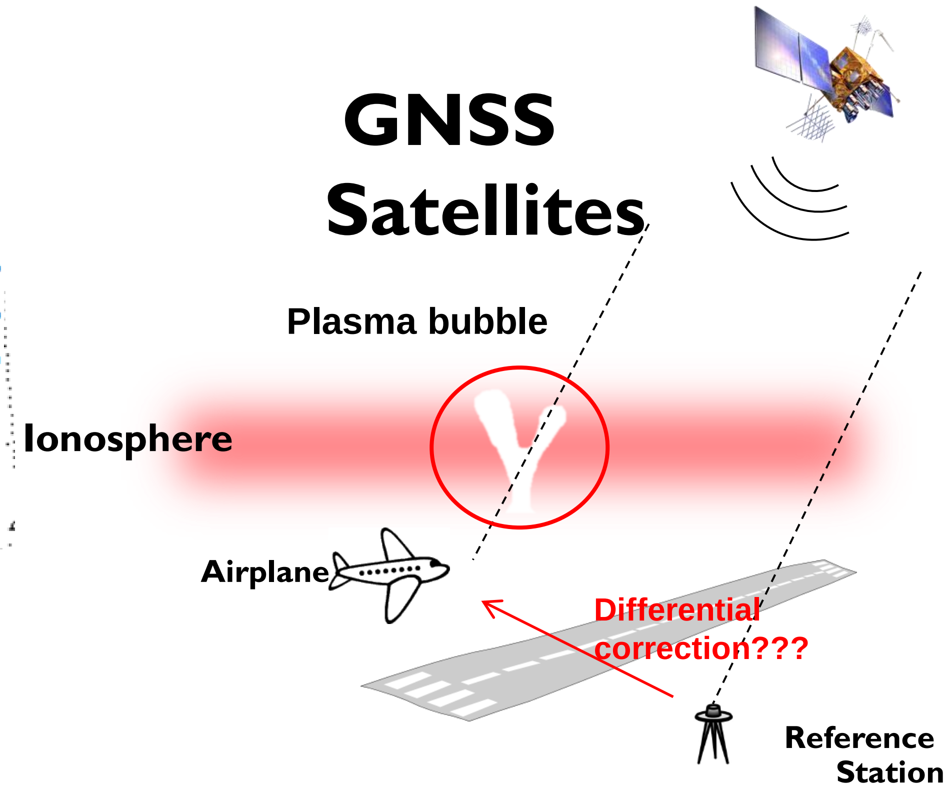

Effects of EPB

Scintillation

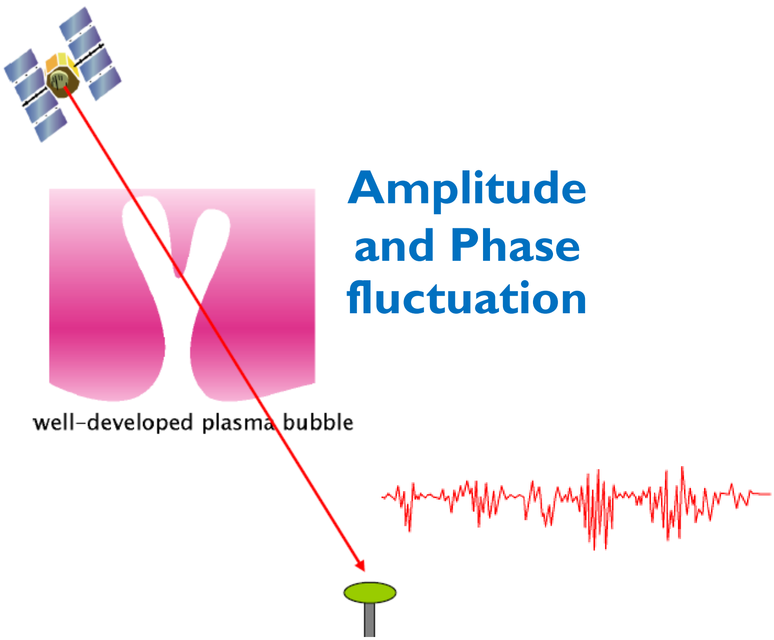

Amplitude and Phase fluctuation

➔ **Loss of lock on GNSS signals**

RTK, PPP-RTK

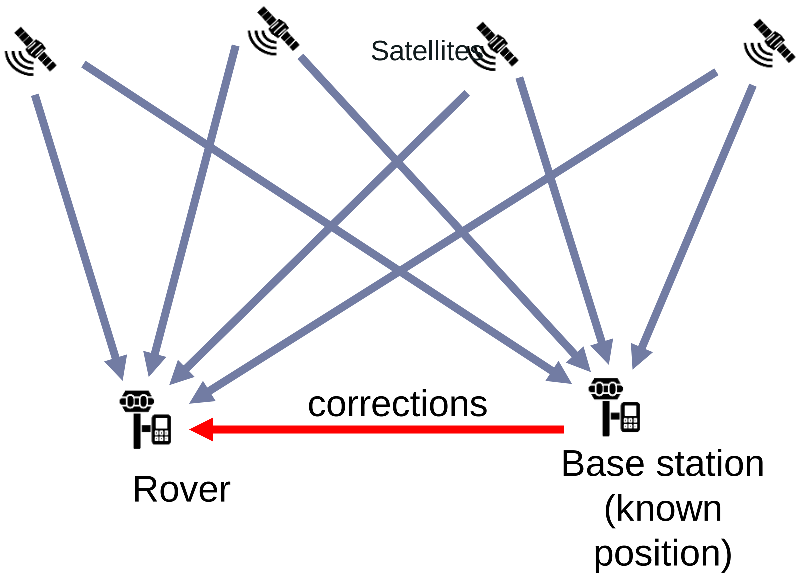

➔ **Increased Positioning errors**

Effects of EPB

HF, VHF Communication

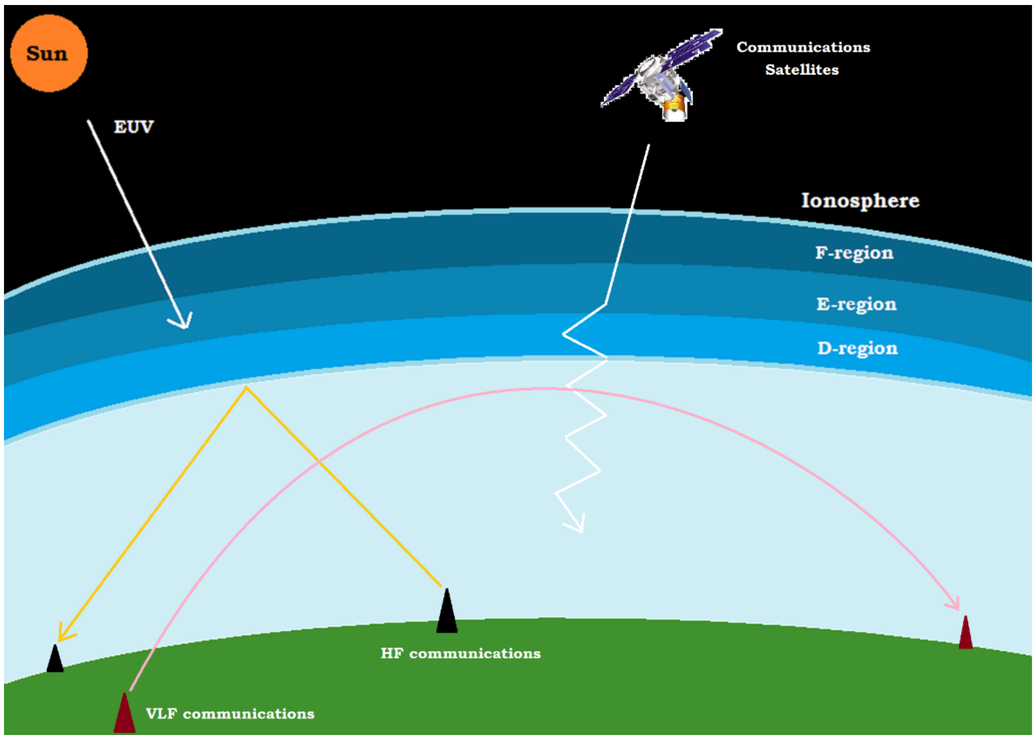


Could Plasma Bubble Have Doomed U.S. Copter in Afghanistan Battle?

A U.S. military rescue mission in Afghanistan went horribly wrong when a crucial radio message wasn't received.

➔ **Communication outage**

https://www.nbcnews.com/science/science-news/could-plasma-bubble-have-doomed-u-s-copter-afghanistan-battle-n214411

Space Weather Products for Aviation

Guidance on Criteria for SW Providers

3-Technical Criteria

a) Ability to provide the space weather information service, both near real-time and forecast information, as defined in the draft SARPs for Amendment 78 of ICAO Annex 3 Meteorological Service for International Air Navigation.

b) Ability to access observations (own observations and received from other space weather providers) of:
  - Coronal mass ejections and high-speed streams
  - Geomagnetic storms
  - Solar radiation storms
  - Solar flares
  - Solar radio bursts
  - Ionospheric activity

c) Ability to produce near real-time and forecast information regarding the potential impacts of space weather using numerical models capable of ingesting observation data from multiple sources.

d) Ability to produce near real-time and forecast information that meets the proposed functional and performance requirements.

e) Ability to coordinate and harmonize information with the space weather information providers for adjacent areas of responsibility, as necessary.

f) Ability to conduct forecast verification

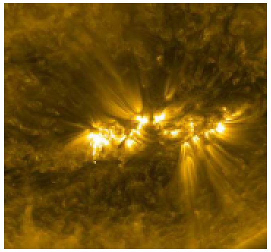

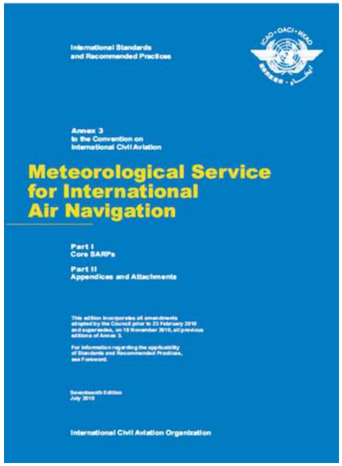

End of 2018 **Early 2019**	Commence production and dissemination of space weather information.

*R. Romero, "Establishment of Space Weather Information Service for International Air Navigation," **UN/USA Workshop on the International Space Weather Initiative, Boston, 31 July- 4 August 2017**.*

Instruments: Optical Sky Imagers

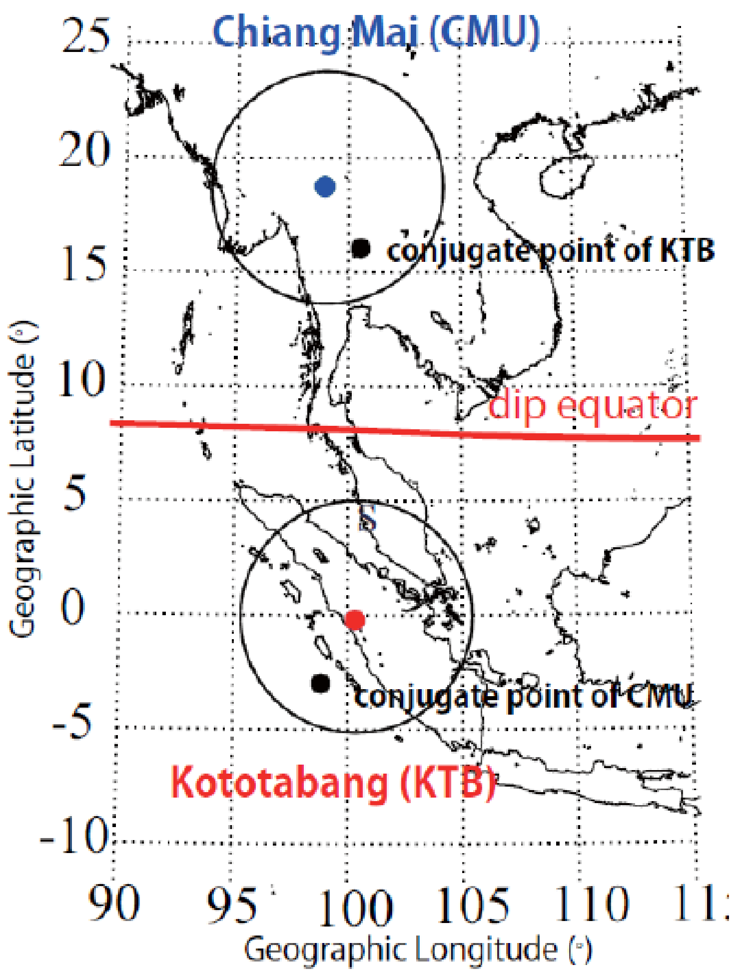

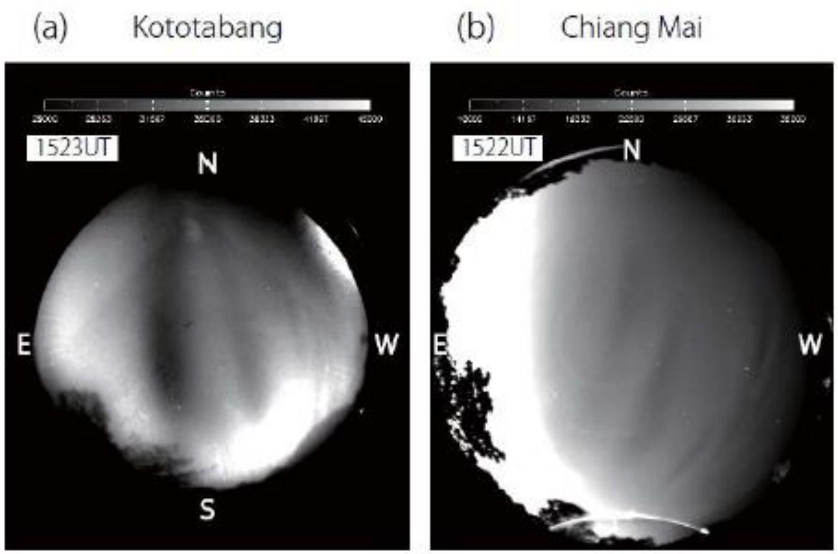

Fukushima et al. (JGR, 2015)

Instruments: GNSS receivers

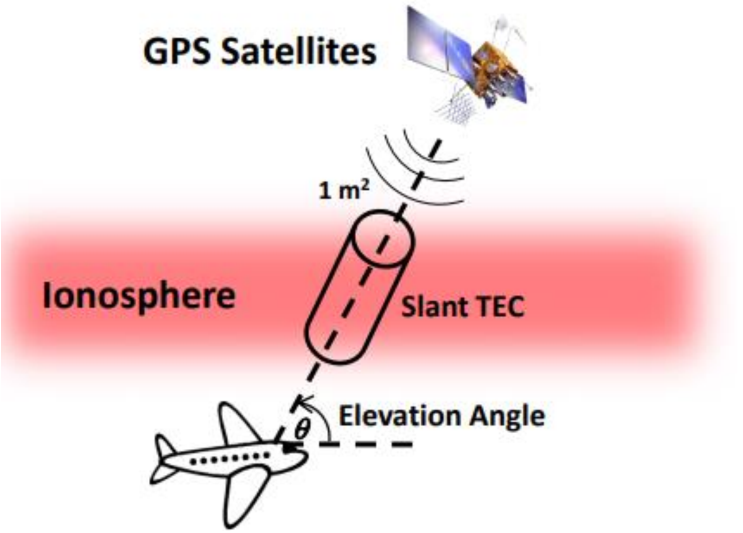

Vertical total electron content (VTEC)

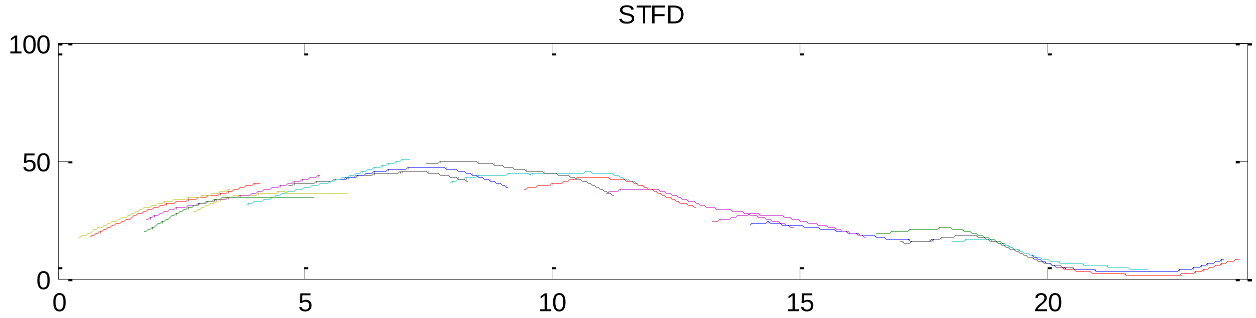

Instruments: Ionosonde

Ionosonde

f = 2 – 30 MHz   Mae-hea, Chiangmai

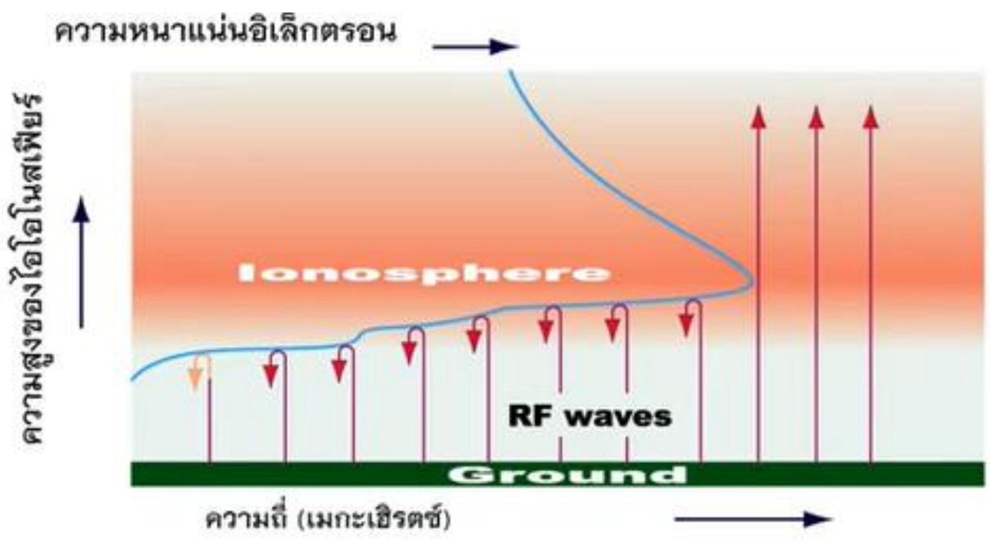

Transmit each frequency upward, then measure the returning echoes.
Measure critical frequencies E, F layer,, heights

Ionograms

Ionograms show traces of echoes (heights) versus frequency (MHz)

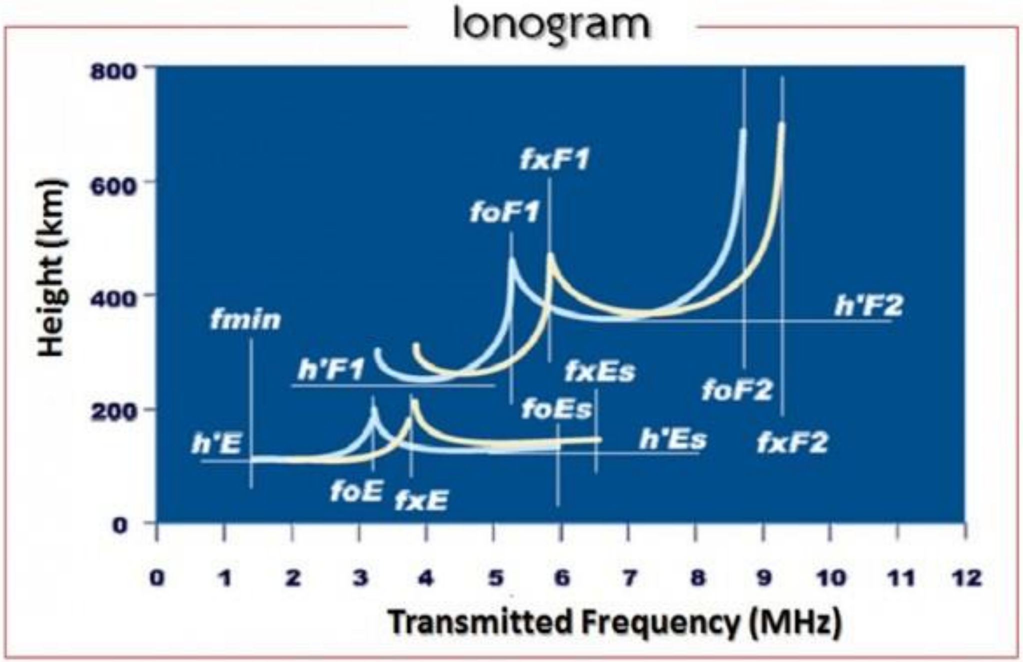

Measure
- foE critical frequency@ E layer
- fof2 critical frequency@ f2 layer
- h'F, h'E (heights-
- Spread F (nighttime)
- Sporadic E (daytime)
- etc.

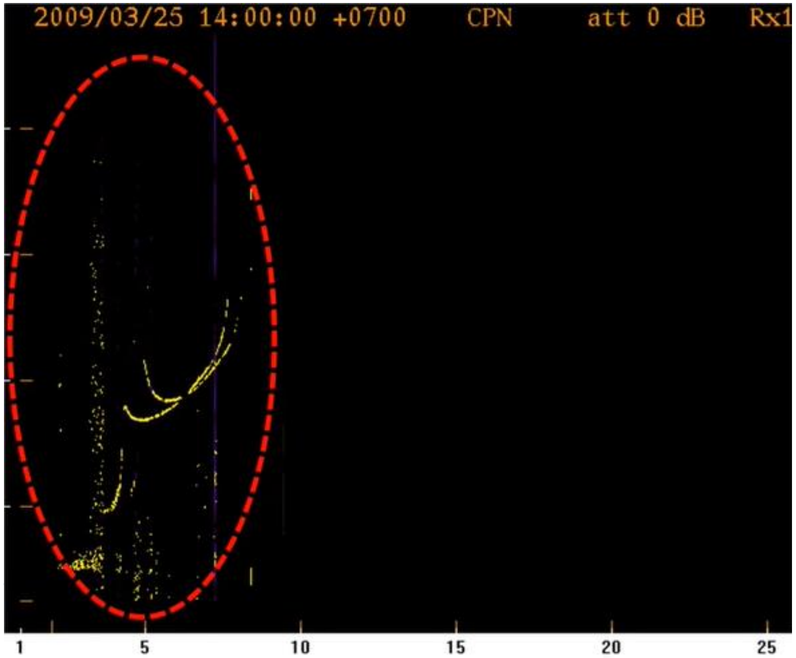

Instruments: Satellites

Beacon satellites

COSMIC/Formosat

Low-earth orbit (LEO) satellites
f = 150,400 MHz

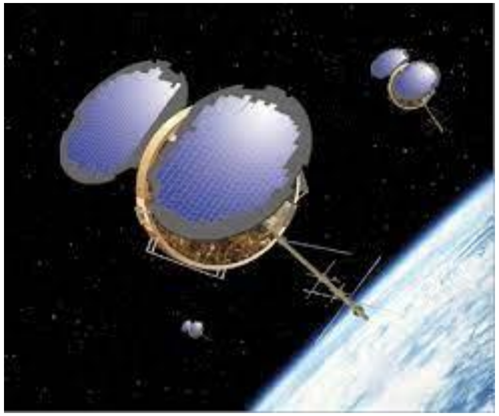

Medium-earth orbit (MEO) satellites
f = GPS frequency

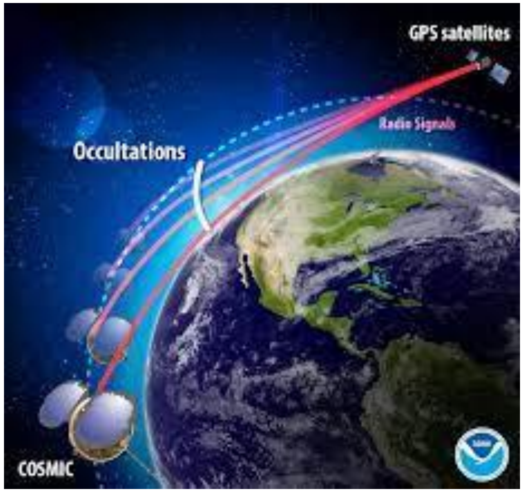

Radio Occultation

Instruments: Incoherent Scatter Radar

Arecibo ISR system Peru)

Aperture diameter - 305 m
Transmit power - 2.5 MW
Frequency
- 430 MHz (original)
- 3 MHz to 10 GHz (upgrade)

Measures
- Electron density (Ne)
- Electron temperature (Te)
- Ion temperature (Ti)

http://www.astronomy.com/media/Images/News%20and%20Observing/News/2016/03/AreciboObservatory.jpg

Ionospheric observeations over Indonesia

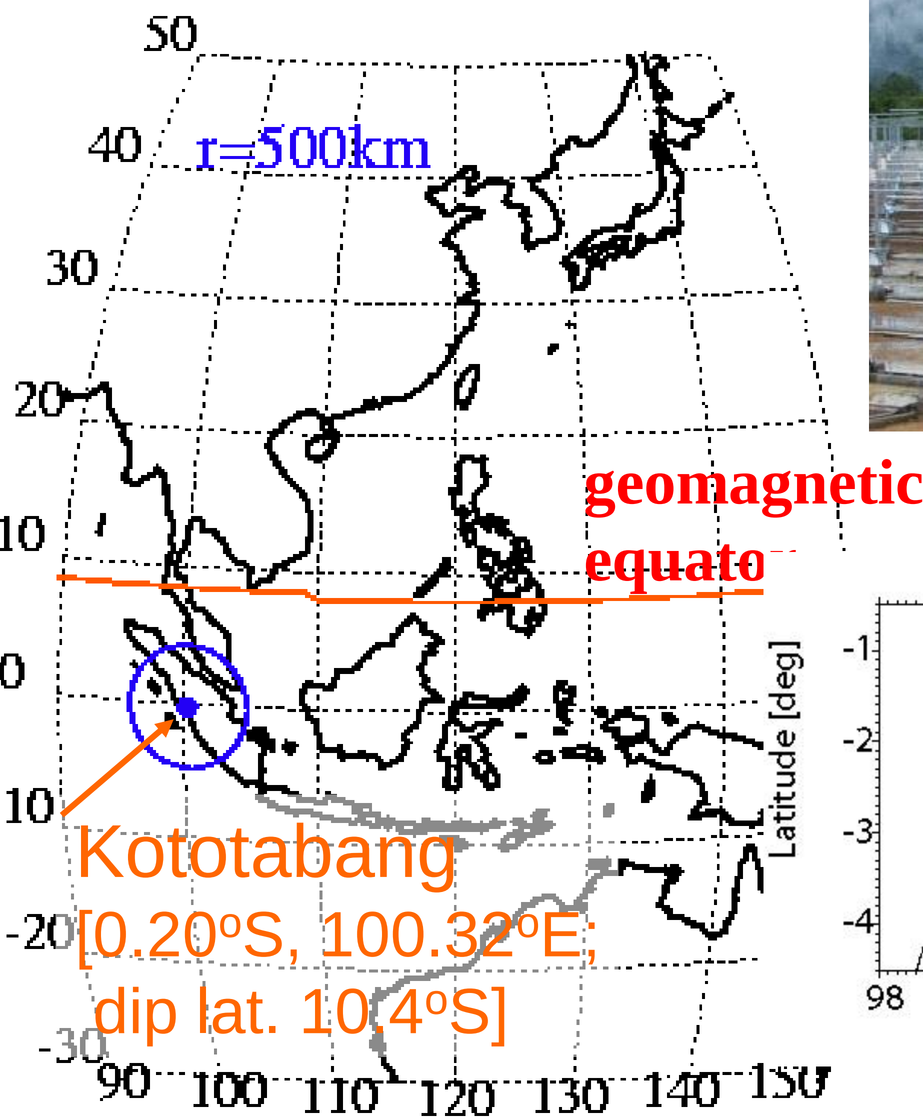

Equatorial Atmosphere Radar (EAR)

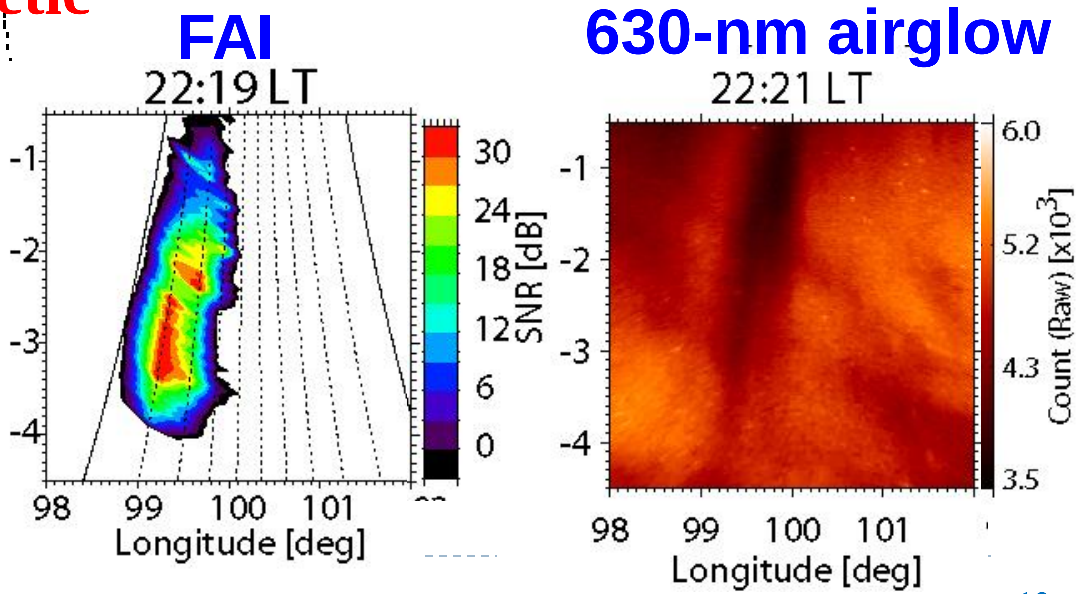

[Otsuka et al., 2004]

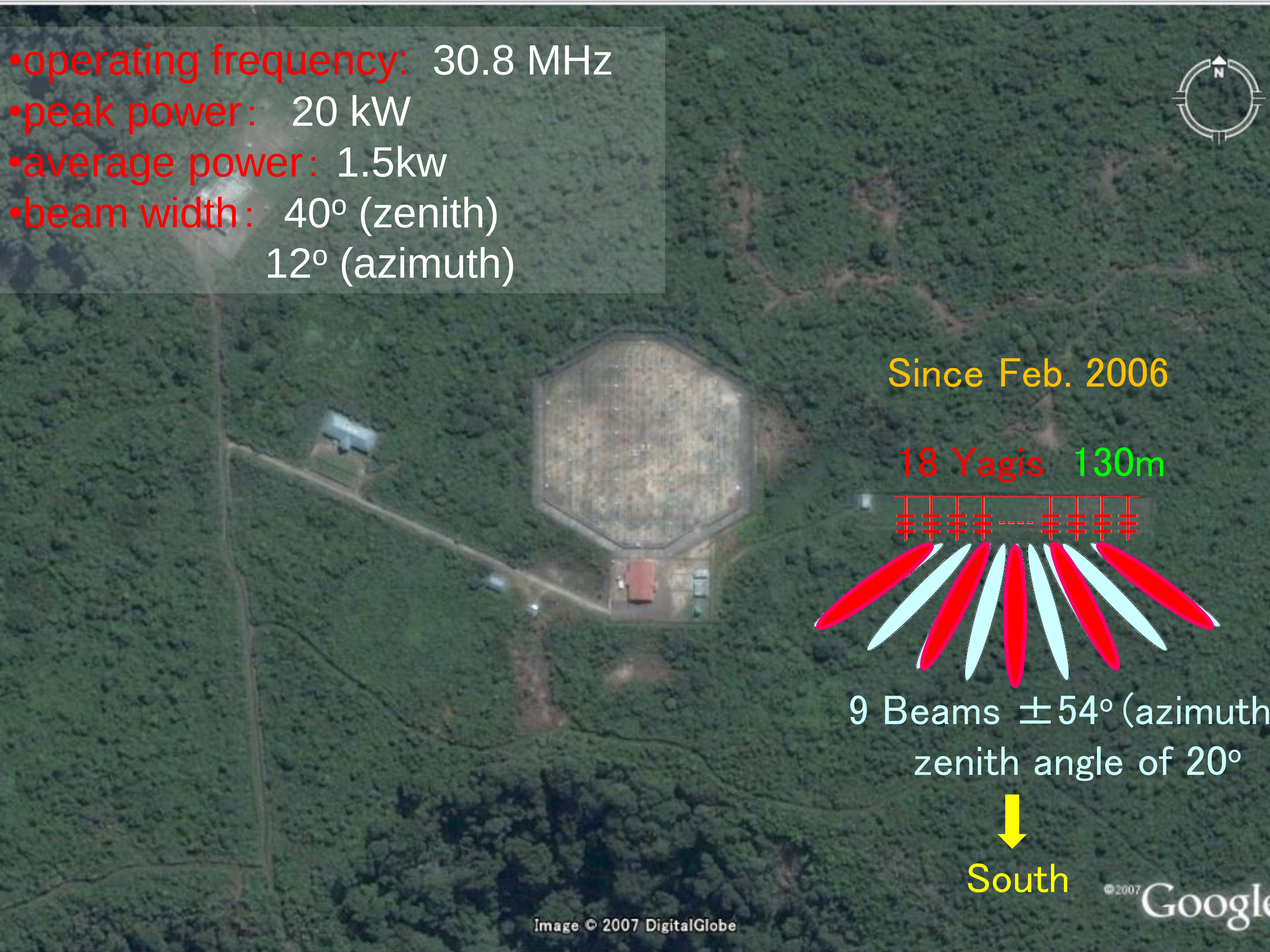
•operating frequency: 30.8 MHz
•peak power: 20 kW
•average power: 1.5kw
•beam width: 40° (zenith)
12° (azimuth)
Since Feb. 2006
18 Yagis 130m
9 Beams ±54° (azimuth
zenith angle of 20°
South
Image © 2007 DigitalGlobe
©2007 Google

Instruments: Chumphon radar station

VHF station

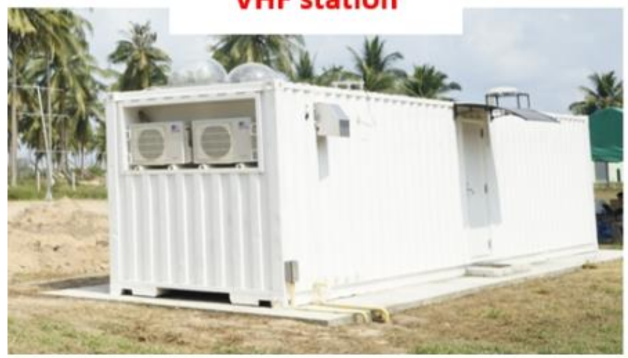

VHF Antenna

Since 2020

Freq. = 39 MHz

Measures the returned echoes and signal strength,

Signal-to-noise ratio (SNR)

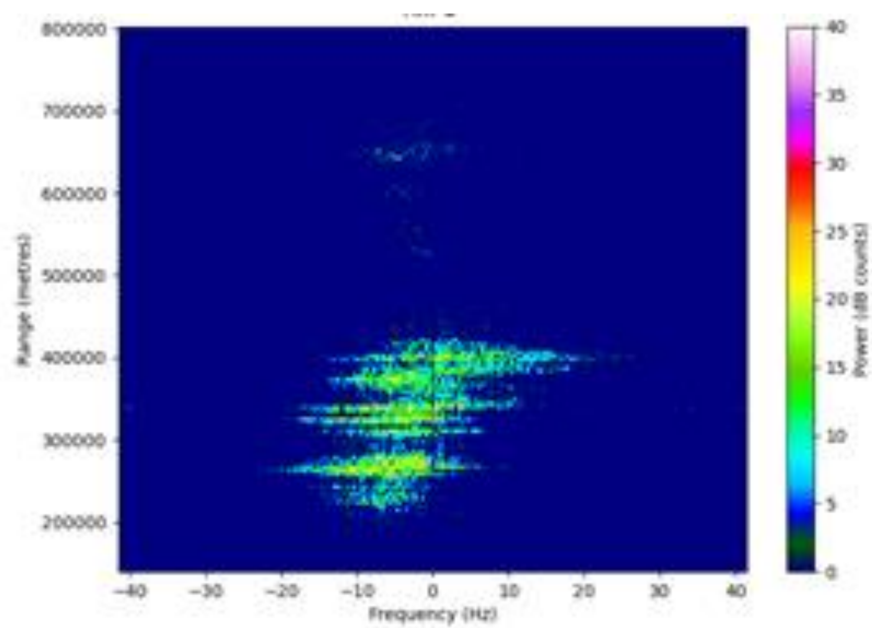

Variability of ESF, EPB

- Long-term variation
  - Pre-reversal enhancement (PRE)
  - solar cycle dependent (F10.7, SSN)
- Medium-term variation
- Short-term or day-to-day variation
  - Due to gravity waves (GW)
  - caused by LSWS in the bottomside F2 layer
  - **Not sufficient understanding**

Long-term variation

EPB on Global UltravioletImager(GUVI)

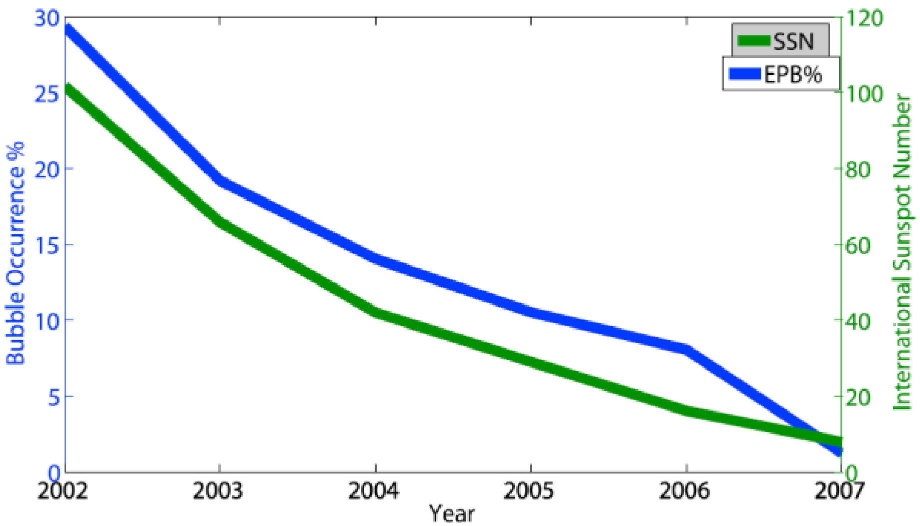

[Comberiate&Paxton,2010]

Optical imager in Brazil

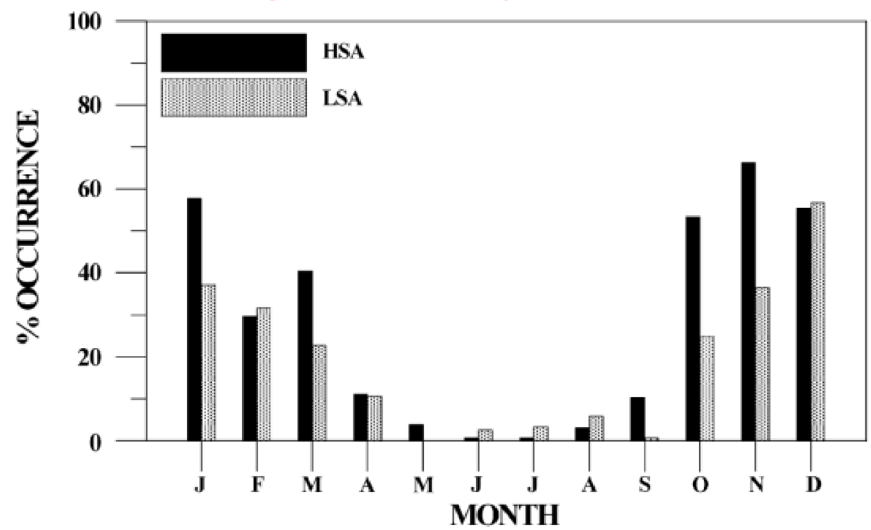

[Sahaietal.,2000]

Annual variation

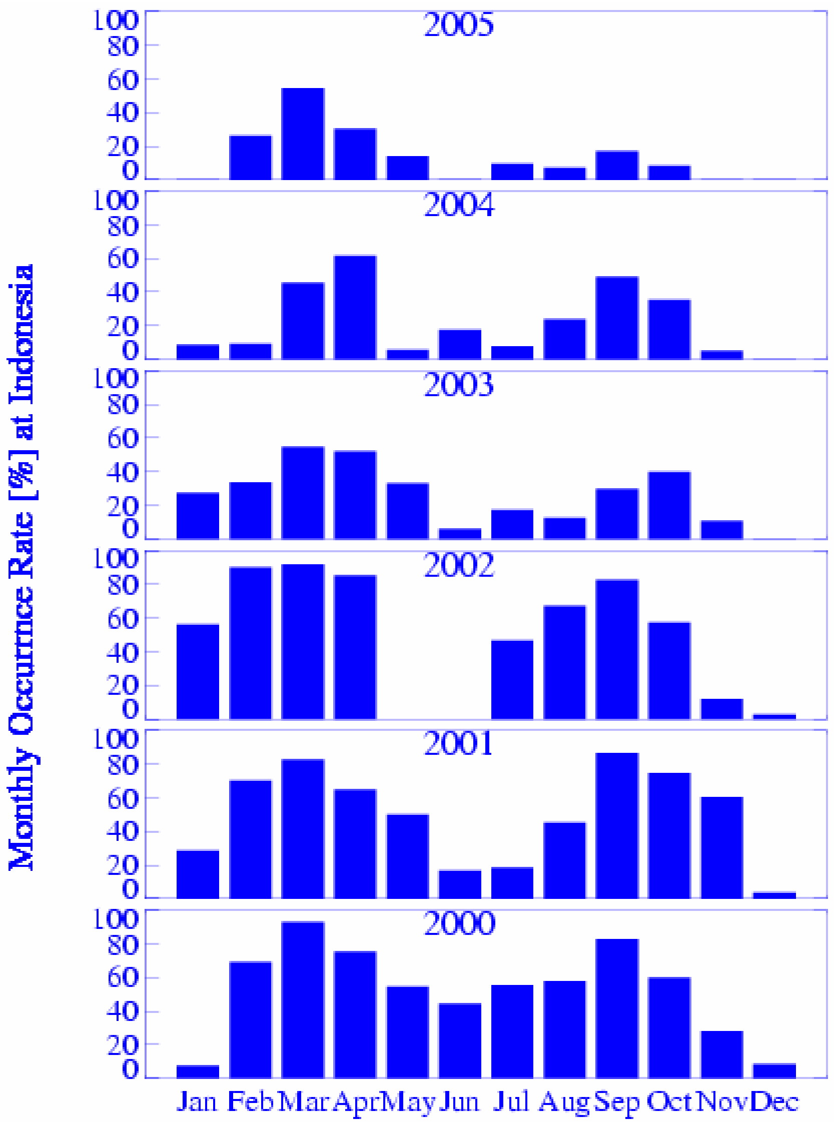

Indonesia

Seasonal variation was repeated in every year.

EPB Occurrence rate was decreasing year by year

Medium-term variation

- Monthly and seasonal scale
- Longitude dependent/magnetic declination/solar declination angle
- The meridional component of the thermospheric wind (The meridional wind)
  - → produce asymmetry in the EIA
  - → increase of the field line integrated conductivity Σ_P
- ESF can be suppressed by meridional winds but if the PRE is large, then ESF can still occur.

Longitudinal dependence of EPB

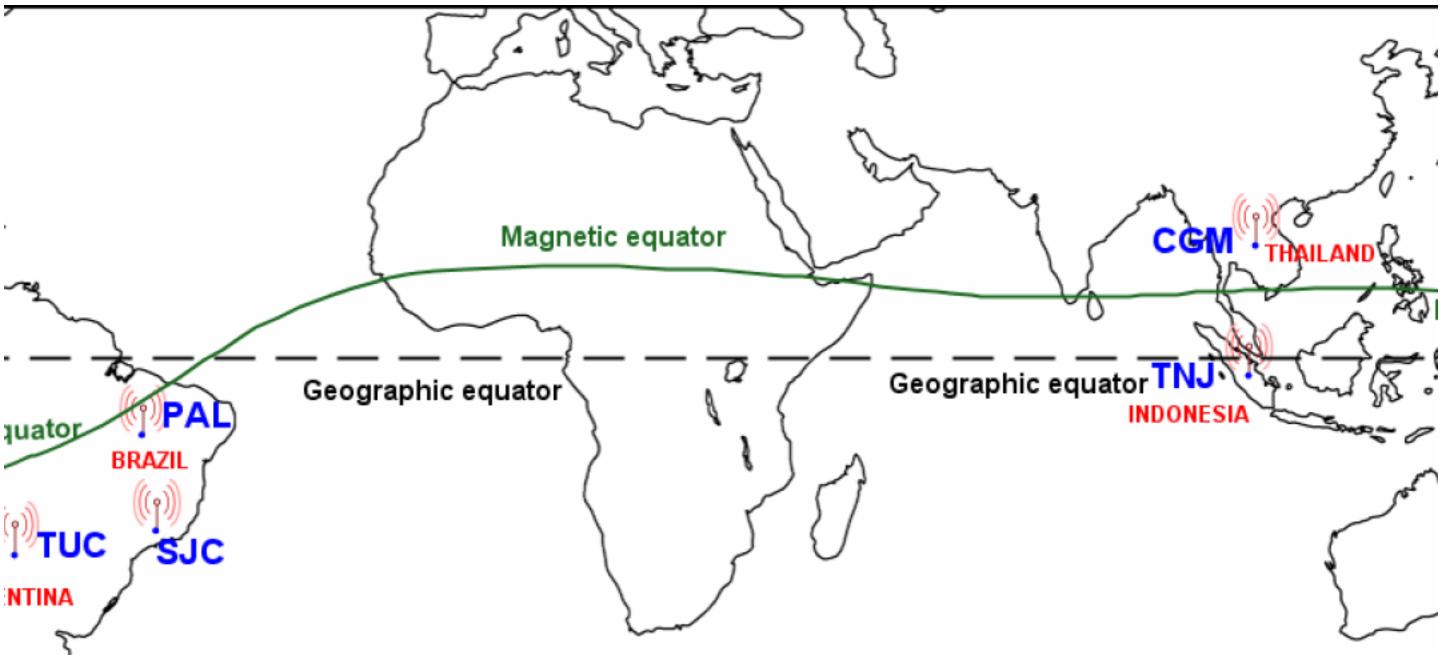

[M. Pezzopane et al., Ann. Geophys., 2013]

Longitudinal dependence of EPB

Chiangmai (18.8ºN, 98.9ºE) **Palmas (10.2ºS, 311.8ºE)**

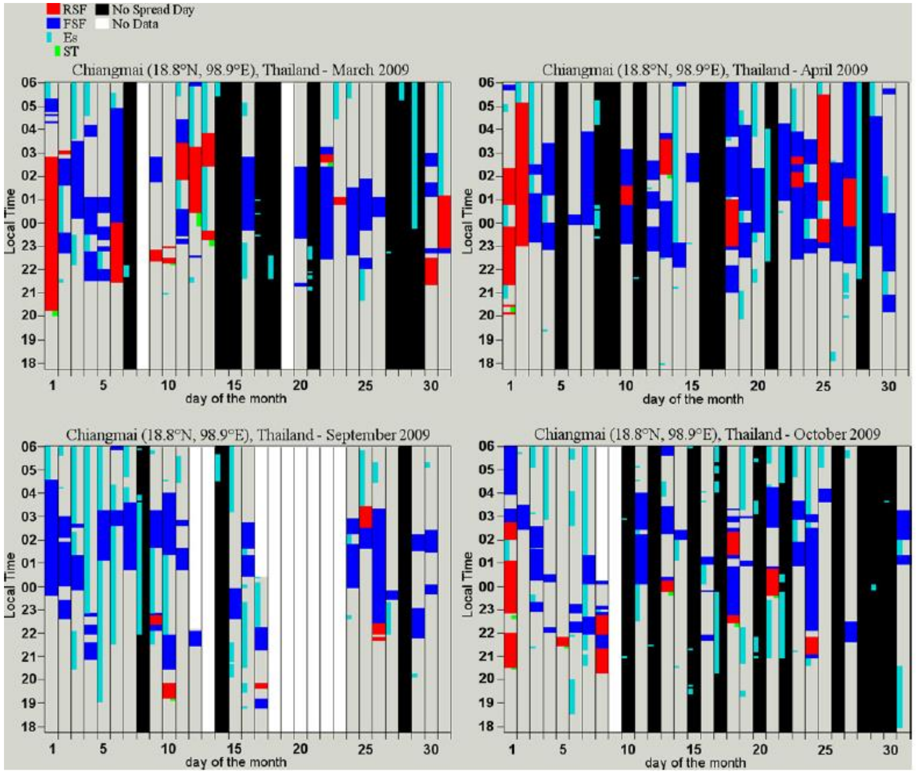

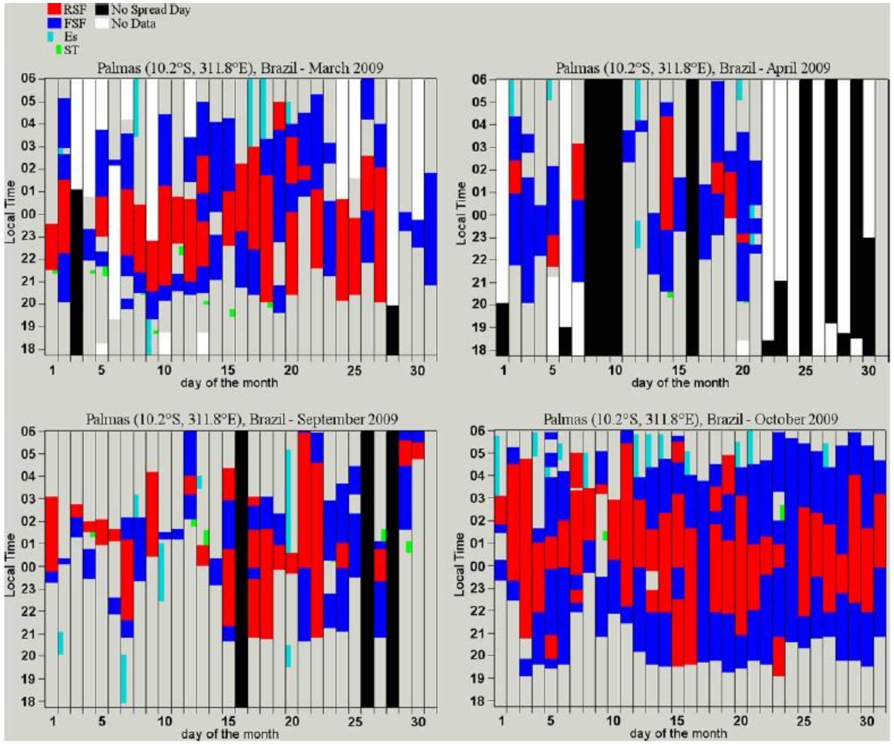

[M. Pezzopane et al., Ann. Geophys., 2013]

In general, %RSF occurrence at CPN is higher than KTB and CMU

This confirms that the plasma bubble is generated around the magnetic equator and then expand to the higher latitude area.

The %RSF occurrence at CMU is not over 20% in average.

2008 **2009**

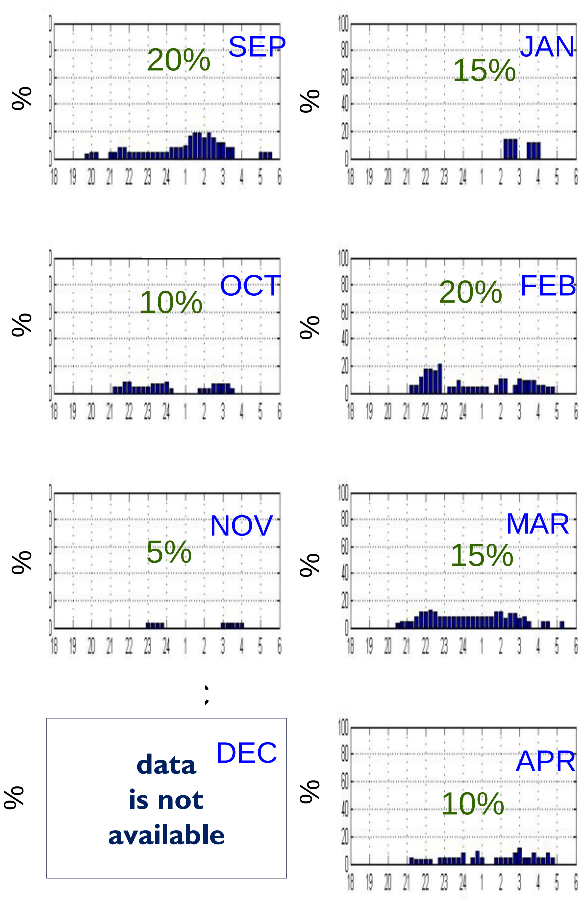

Chumphon (CPN)

The %RSF is not over 20% in averag at CPN in NOV, DEC, JAN and FEB

The higher rate mostly occurs during the equinoctial months

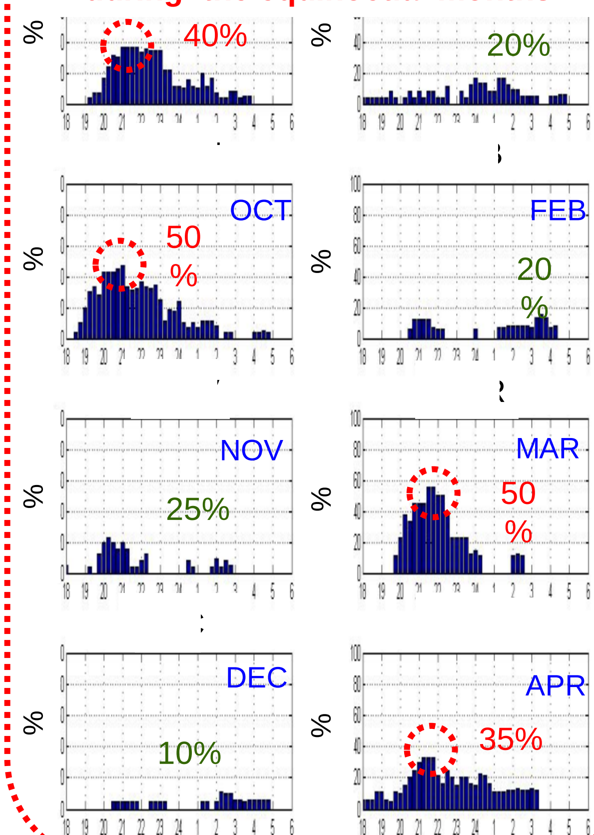

Kototabang (KTB)

The %RSF is not over 20% in average at KTB from OCT to JAN and APR

The higher rate occurs in SEP, FEB and MAR

2008 **2009**

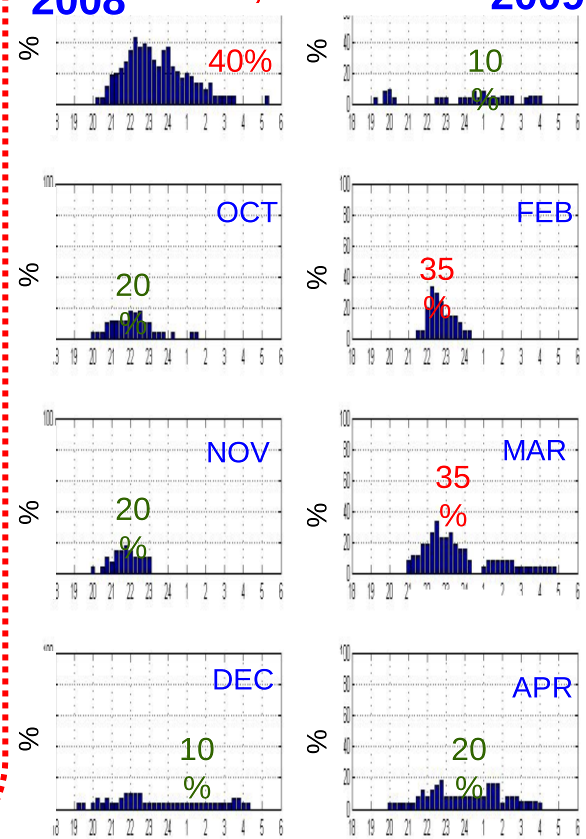

SEALION Project (2005-Present)

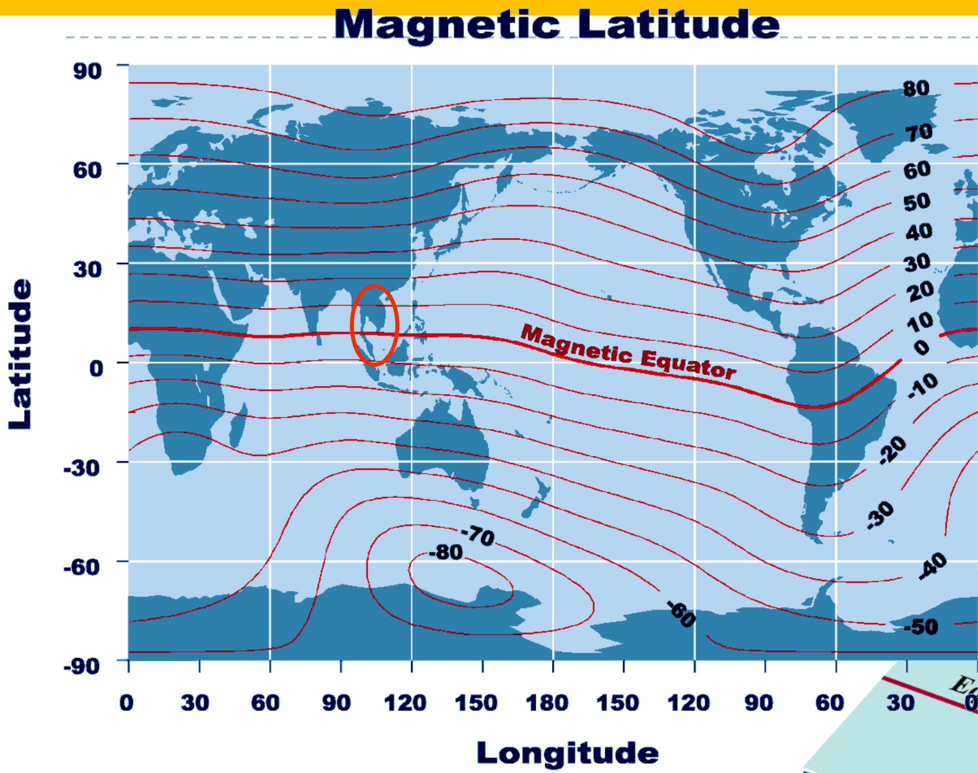

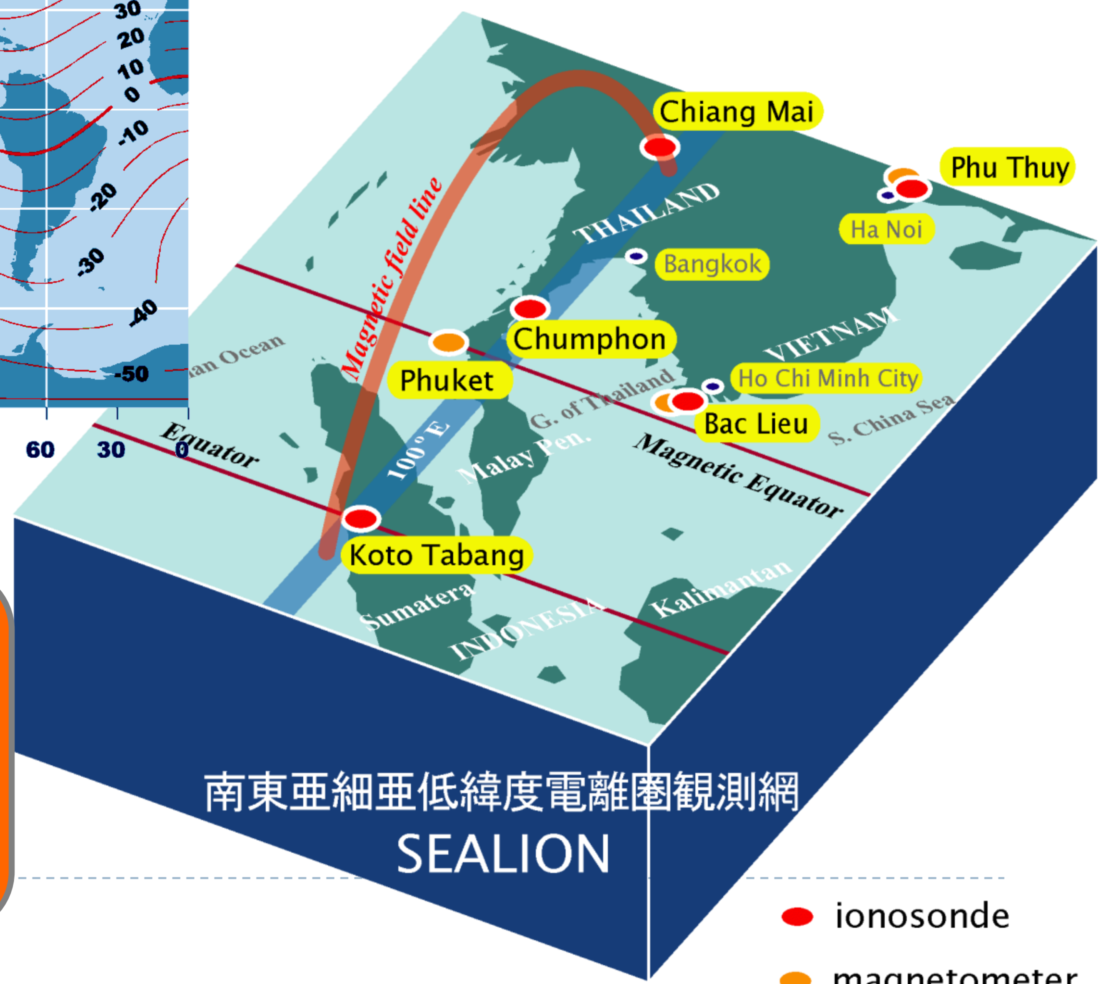

SEALION (South East Asia Low-latitude Ionospheric Network) is an ionospheric observation network in Southeast Asia which has been conducted by National Institute of Information and Communication Technology **(NICT)**, Japan

GBAS Project (2011-Present)

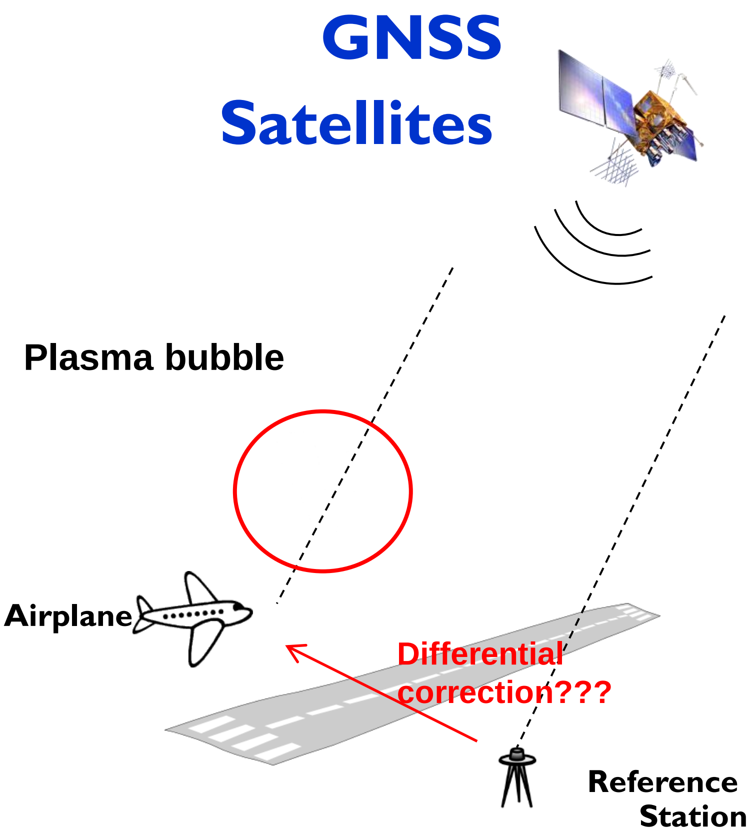

ENRI

บริษัท วิทยุการบินแห่งประเทศไทย จำกัด
AERONAUTICAL RADIO OF THAILAND LTD.

KMITL
พระจอมเกล้าลาดกระบัง

Goals:

1. to study statistics of delay gradients in the ionosphere during quiet time and disturbed time
2. To evaluate GBAS performance (CAT-I, II, III)

Thai GNSS&Space Weather Information Center

http://iono-gnss.kmitl.ac.th/

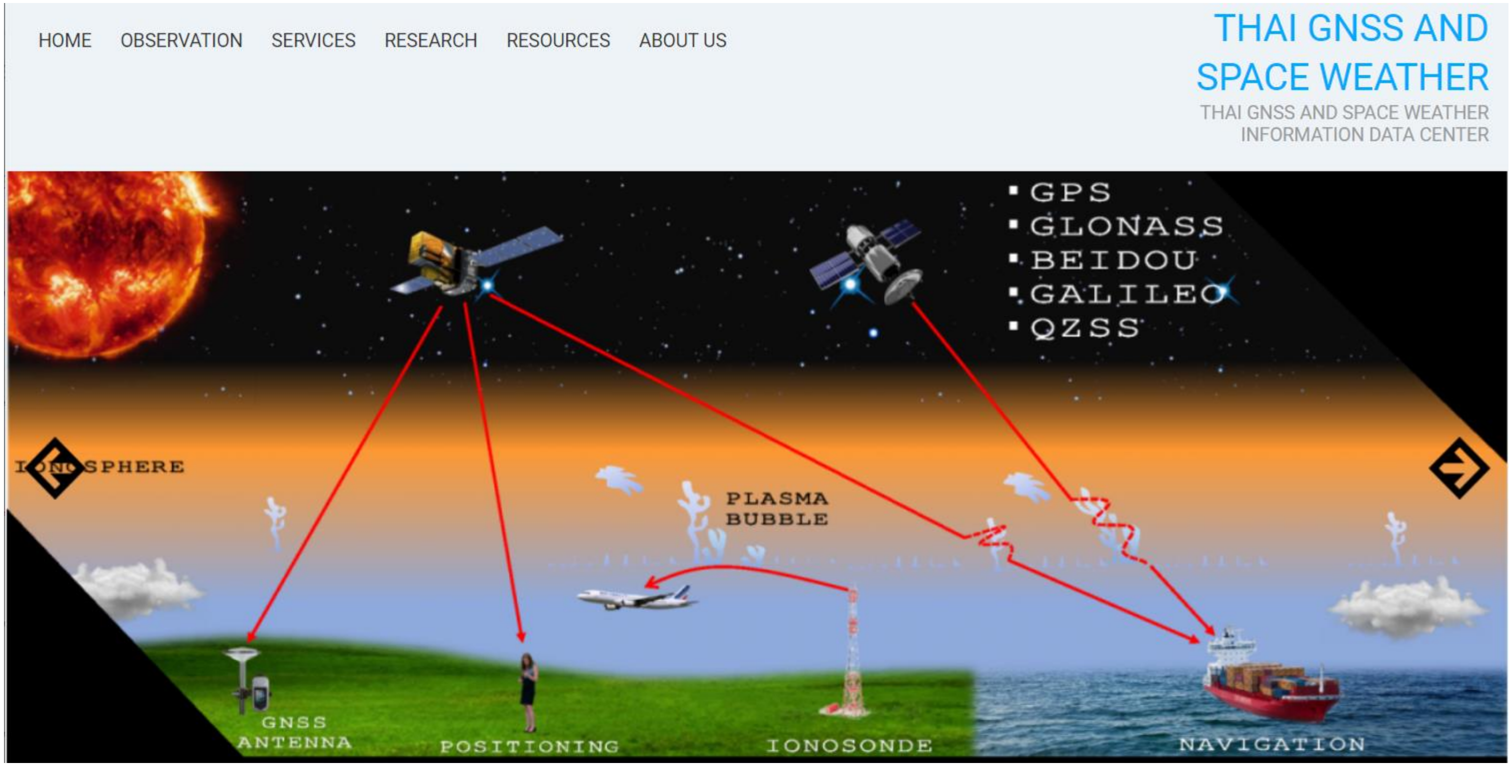

Computing Total Electron Content with Data from GNSS receiver

GPS

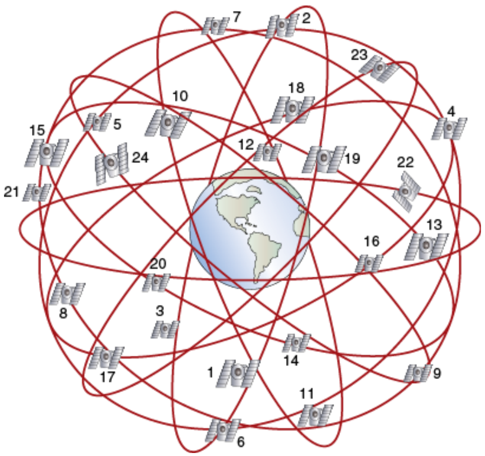

Galileo

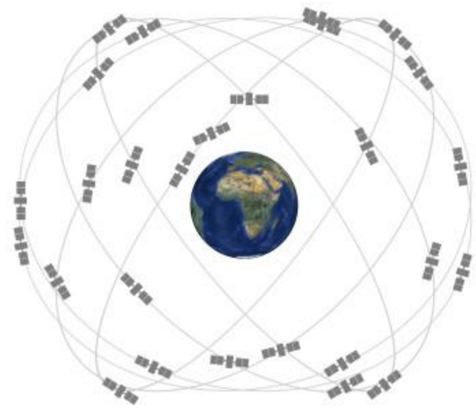

Beidou
(Compass)

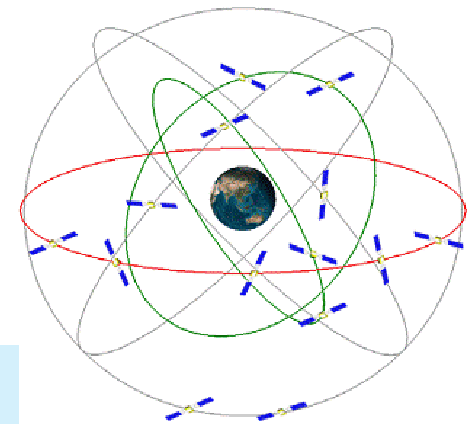

Glonass

QZSS

Time delay due to ionosphere

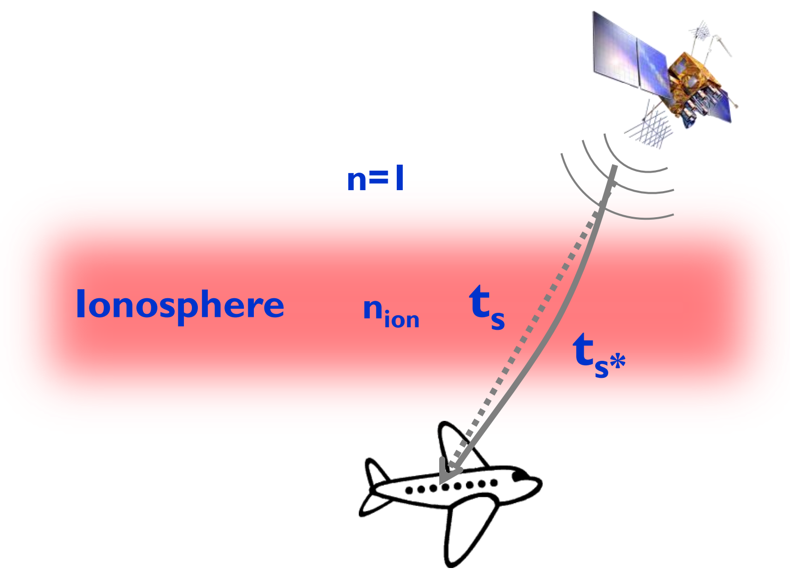

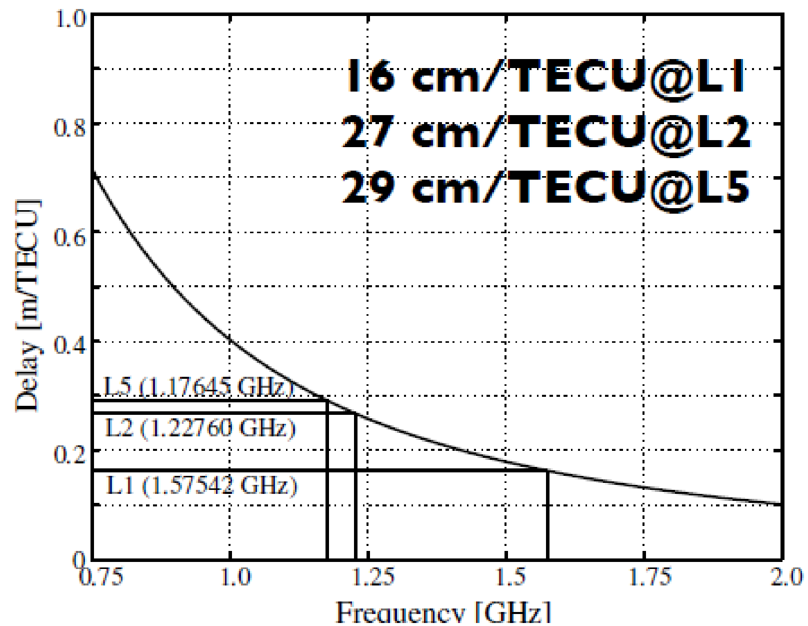

Ionospheric delay:

$$I = c \times \delta t = \frac{40.3}{f^2} TEC$$

(meter)

Ex. At 1.57542 GHz (GPS L1), 16 cm delay per 1 TECU ($10^{16} m^{-2}$)

- Pseudorange (R) can be computed from 'code' or 'carrier phase'

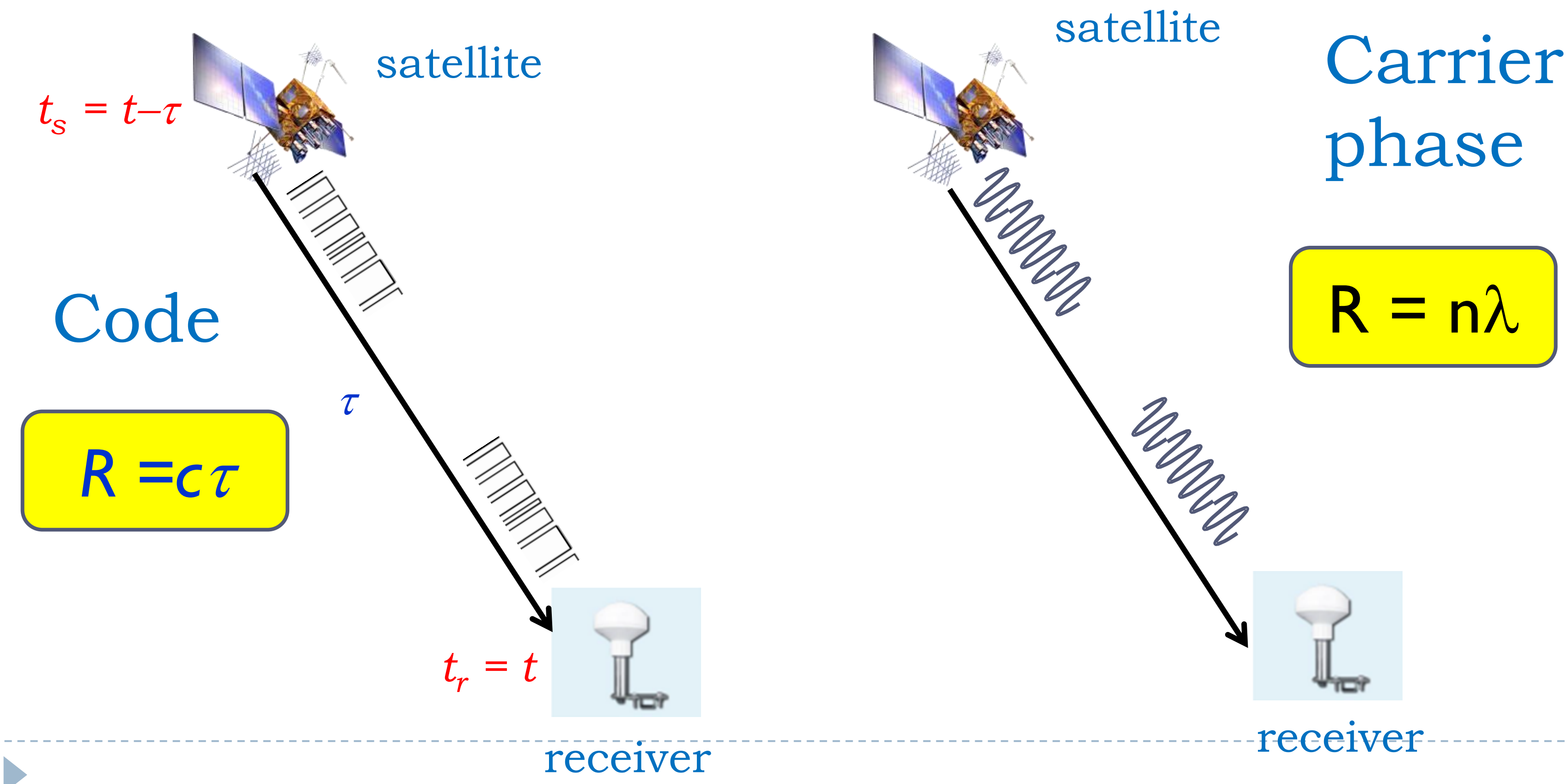

Slant TEC (STEC)

= delay in satellite signal on the slant path

Pseudorange : $STEC_P = k(P_2 - P_1)$

Carrier phase : $STEC_L = k(L_1 - L_2)$

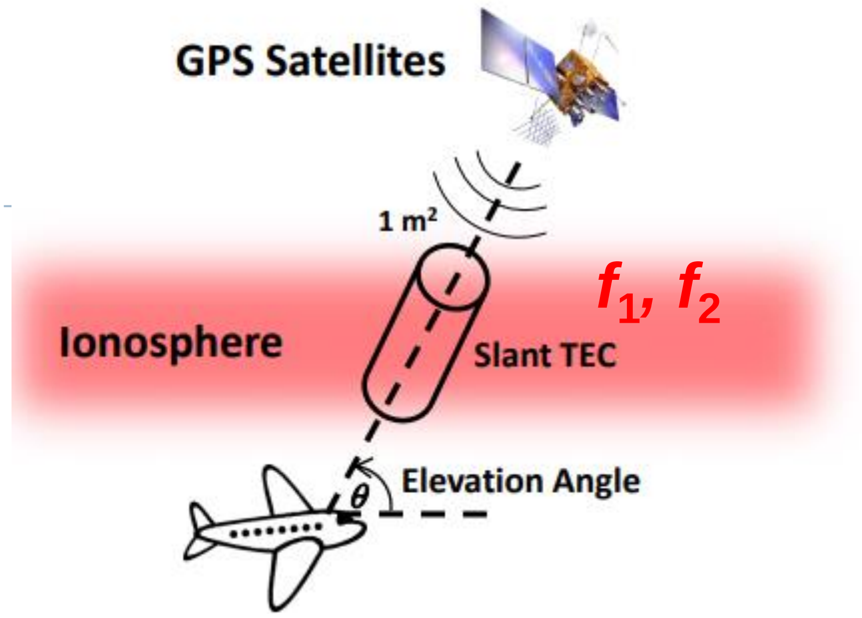

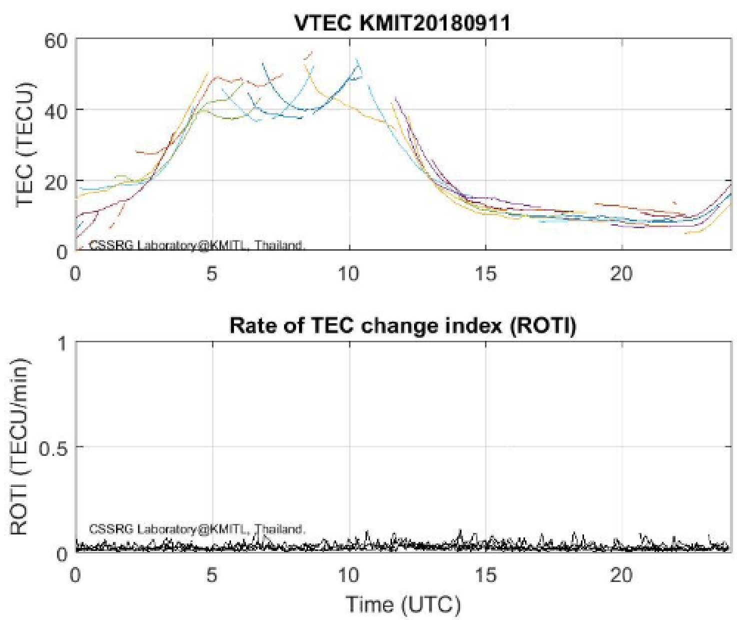

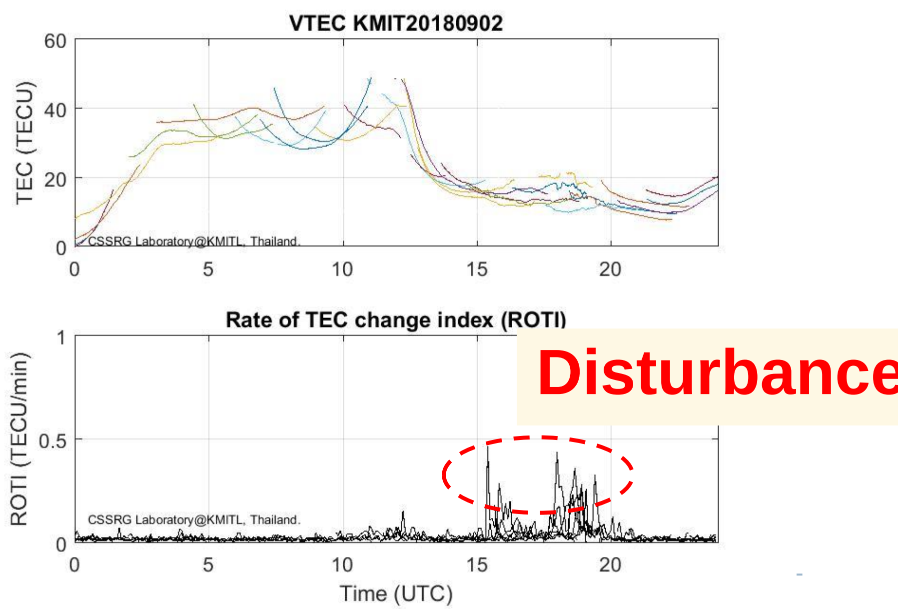

GNSS observation system

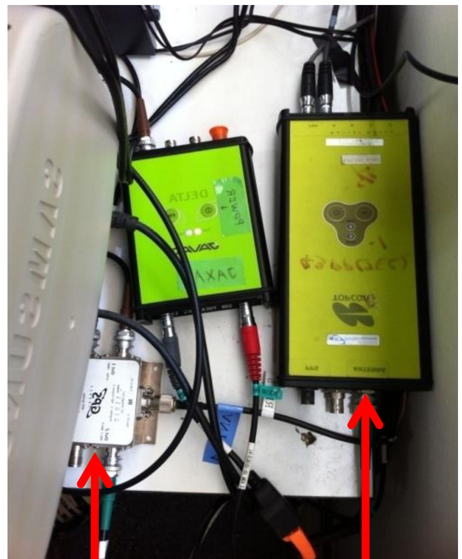

สายอากาศ GNSS

อุปกรณ์แยกสัญญาณ (Splitter)

เครื่องรับ GNSS

เครื่องคอมพิวเตอร์ที่ใช้ระบบปฏิบัติการ Linux

RINEX Observation File

```
     2.11           OBSERVATION DATA    G (GPS)             RINEX VERSION / TYPE
teqc  2010Oct21                         20101216 08:31:59UTCPGM / RUN BY / DATE
DPT9                                                        MARKER NAME
DPT9                                                        MARKER NUMBER
SURVEY DIV          DPT SURVEY DIV                          OBSERVER / AGENCY
462972              LEICA GRX1200PRO    4.12/2.121          REC # / TYPE / VERS
                    LEIAT502        NONE                    ANT # / TYPE
 -1136984.0551  6091176.7425  1506867.1803                  APPROX POSITION XYZ
        0.0000        0.0000        0.0000                  ANTENNA: DELTA H/E/N
     1     1                                                WAVELENGTH FACT L1/2
     4    C1    L1    P2    L2                              # / TYPES OF OBSERV
     5.0000                                                 INTERVAL
    15                                                      LEAP SECONDS
Linux 2.4.20-8|Pentium IV|gcc -static|Linux|486/DX+         COMMENT
     2.10           OBSERVATION DATA    G                   COMMENT
SPIDER V2,1,0,2275                      2010 10 03 01:00    COMMENT
BIT 2 OF LLI FLAGS DATA COLLECTED UNDER A/S CONDITION       COMMENT
SNR is mapped to RINEX snr flag value [2-9]                 COMMENT
L1&L2:  = 25dBHz -> 1; 26-27dBHz -> 2; 28-31dBHz -> 3       COMMENT
       32-35dBHz -> 4; 36-38dBHz -> 5; 39-41dBHz -> 6       COMMENT
       42-44dBHz -> 7; 45-48dBHz -> 8; >=49dBHz -> 9        COMMENT
  2010    10     3     0     0    0.0000000     GPS         TIME OF FIRST OBS
                                                            END OF HEADER
 10 10  3  0  0  0.0000000  0  9G03G06G14G16G19G20G23G31G32
  21099468.684   110878445.832 8  21099469.730    86398792.12046
  20867624.156   109660094.587 8  20867625.033    85449416.37646
  23455038.256   123257096.017 5  23455039.217    96044496.36343
  20879213.184   109721010.465 8  20879213.310    85496892.40246
  23486877.263   123424370.220 6  23486876.034    96174822.65343
  22092147.352   116095001.410 7  22092146.749    90463636.47745
  23093968.253   121359611.154 6  23093966.845    94565929.26643
  23522597.394   123612102.994 6  23522597.247    96321126.70344
  21549251.572   113242062.708 8  21549252.014    88240570.79145
```

Header Section

Data Section

C1 L1 P2 L2

How to derive TEC from GPS data?

Step 1

Pseudorange : $STEC_P = k(P_2 - P_1)$

Carrier phase : $STEC_L = k(L_1 - L_2)$

Step 2

where k=9.5196 for TEC expressed in TECU.

- **Since the $STEC_P$ is nosier than $STEC_L$ but the $STEC_L$ still has an initial ambiguity which frequently causes the $STEC_L$ to have negative values.**
- **Generally, $STEC_L$ is adjusted to $STEC_P$ level.**

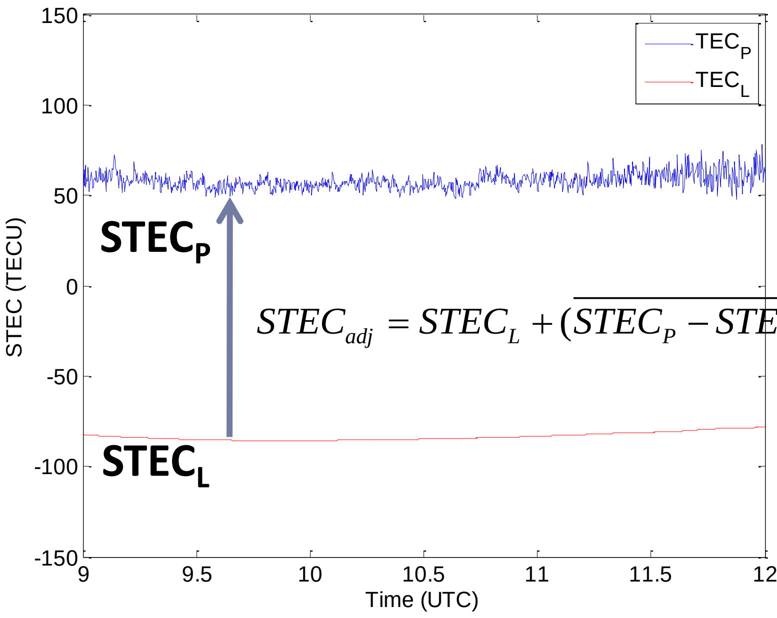

$$STEC_{adj} = STEC_L + \overline{(STEC_P - STEC_L)}_{arc}$$

$$STEC_{adj} = STEC + B_S + B_R$$

Satellite IFB

Receiver IFB

Step 3

Step 4

obtained from IGS by CODE
(Center for Orbit Determination in Europe)

STEC Characteristics

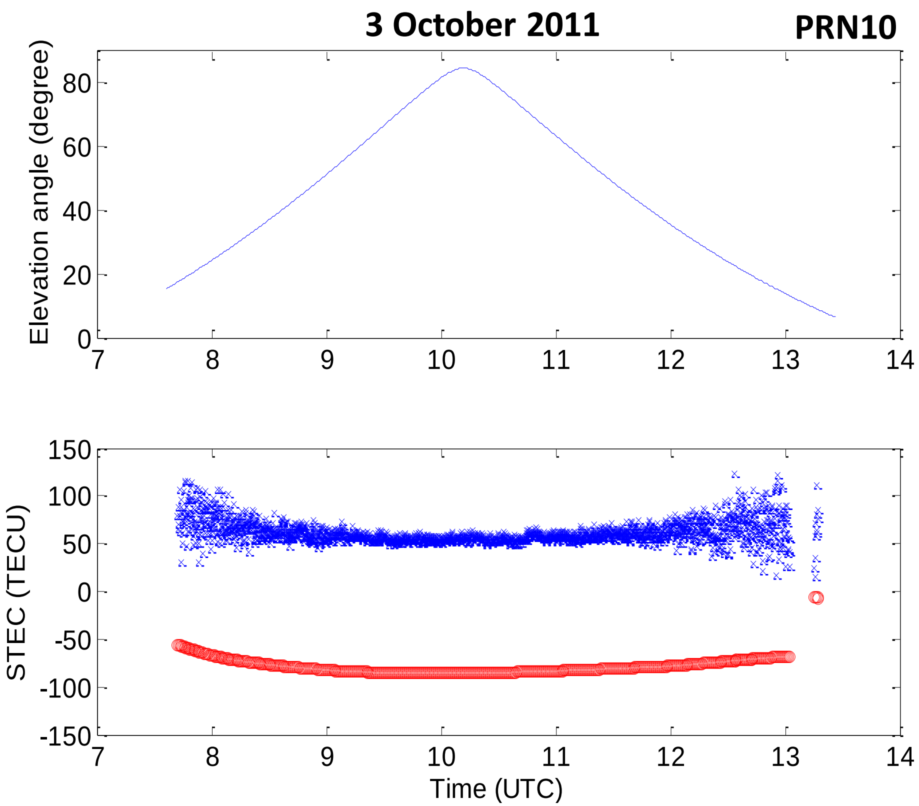

Sky plot

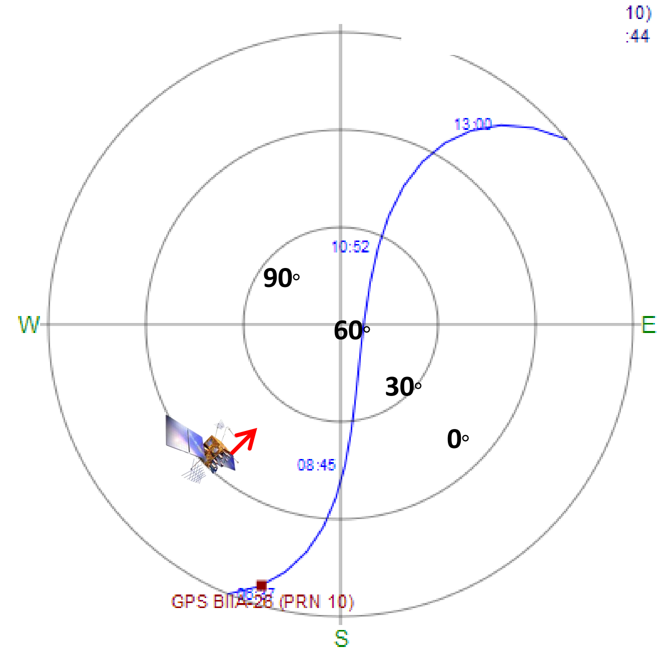

- **The $STEC_P$ become noisy and the $STEC_L$ jumps at low elevation angle.**

- **The TEC_L jumps is due to the cycle slips in the carrier phase measurement, often seen at the low elevation angles.**

Vertical TEC (VTEC) Conversion

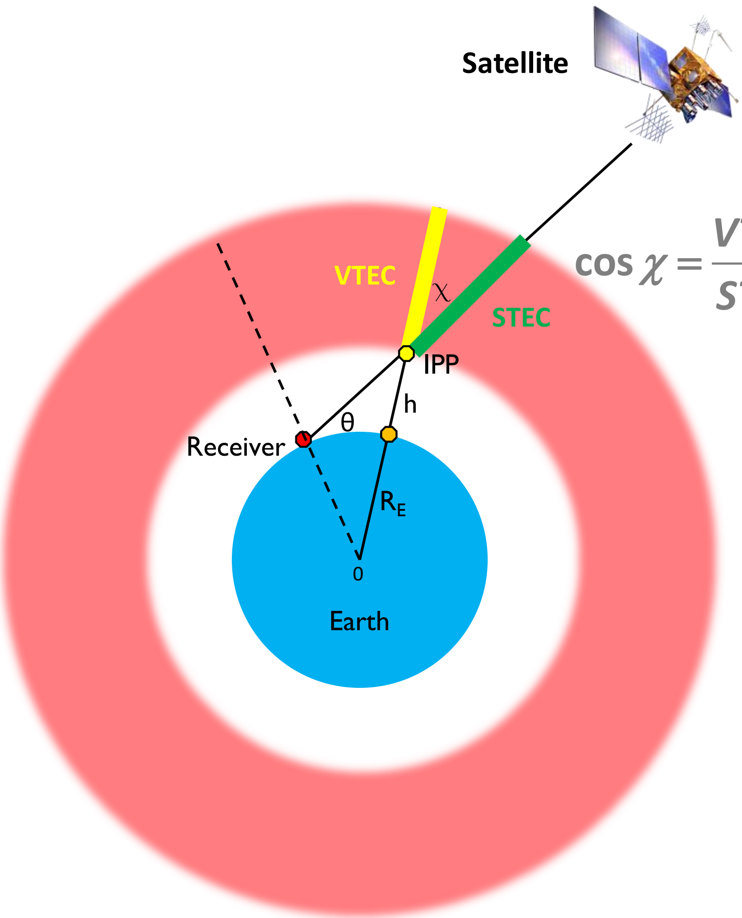

$$\cos\chi = \frac{VTEC}{STEC}$$

- **Single Layer Ionospheric Model (SLIM)**

$$VTEC = STEC\cos\chi$$

$$\cos\chi = \sqrt{1-\left(\frac{R_E}{R_E+h}\cos\theta\right)^2}$$

R_E : Earth's radius (6378.137 km :WGS-84)
h : height of the iospheric layer
θ : Satellite's elevation angle
χ : Zenith angle

STEC : Slant TEC
VTEC : Vertical TEC
IPP : Ionospheric pierce point

STEC vs. VTEC

STEC = Slant TEC

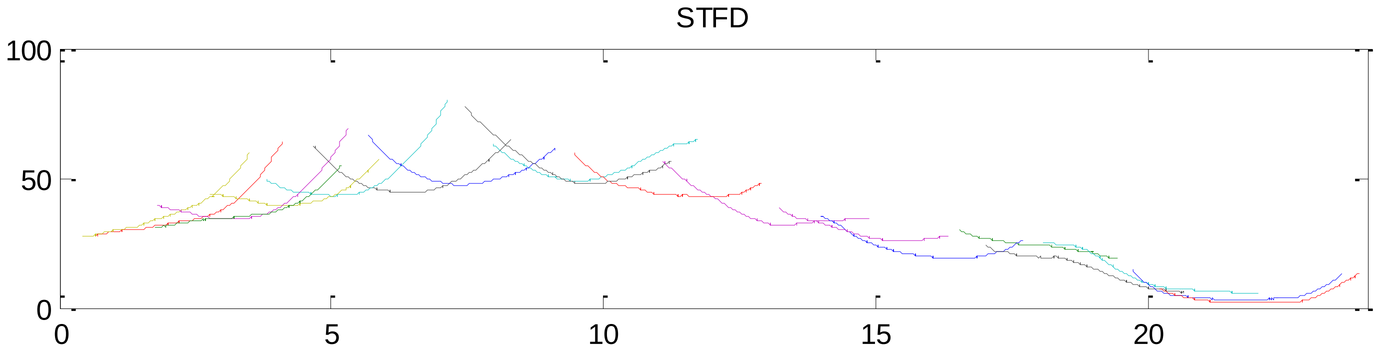

VTEC = Vertical TEC

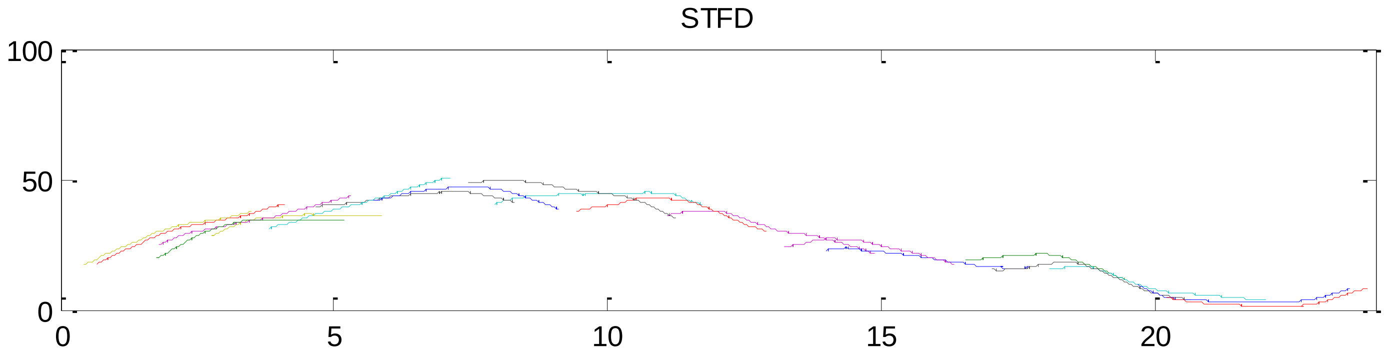

Rate of TEC change index: ROTI

- The ROTI is used for ionospheric irregularities detection at one station for one day, defined by Standard deviation of rate of TEC change with 5-minute windows. In this work, we determined 0.5 TECU/min is the threshold.

$$ROT(i) = STEC(i+1) - STEC(i)$$

$$ROTI = \sqrt{\frac{1}{N}\sum_{i=1}^{N}\left(ROT(i) - \overline{ROT}\right)^2}$$

- i = Index of time
- N = Window times (minutes)

STEC and ROTI at KMITL station

25th September 2012

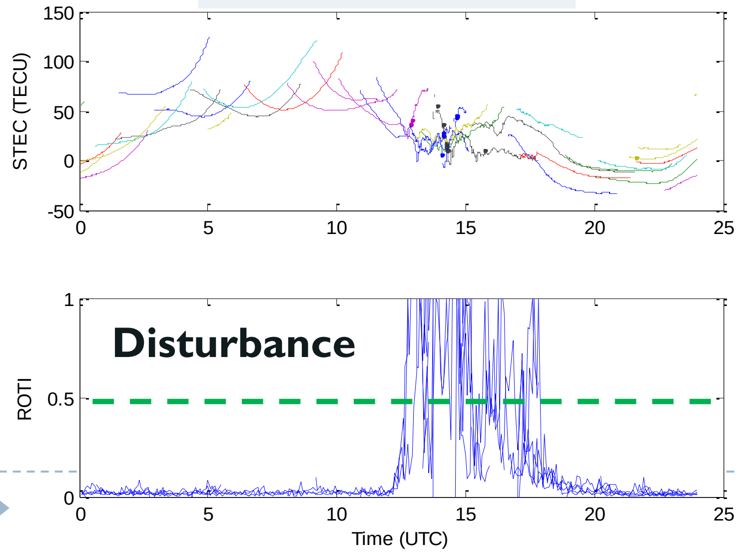

4st August 2012

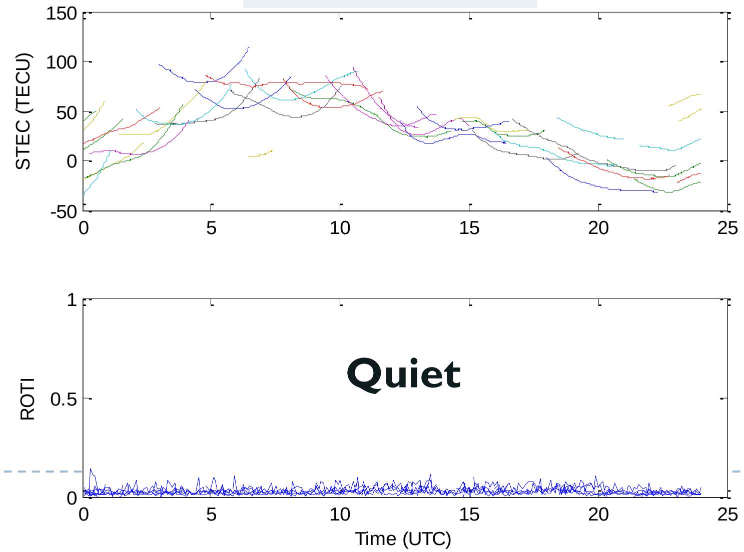

GPS observation

Bangkok area

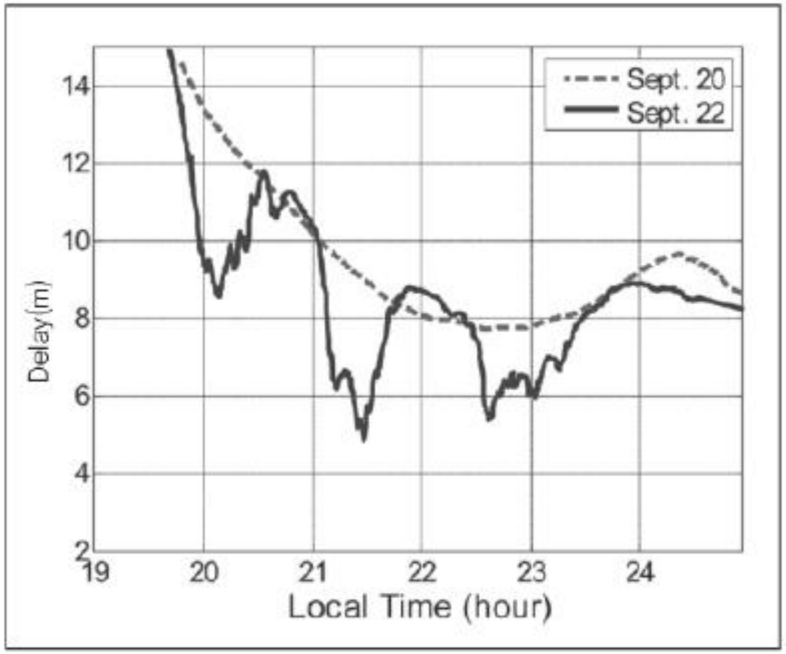

22 Sept. 2011 (uncalibrated TEC)

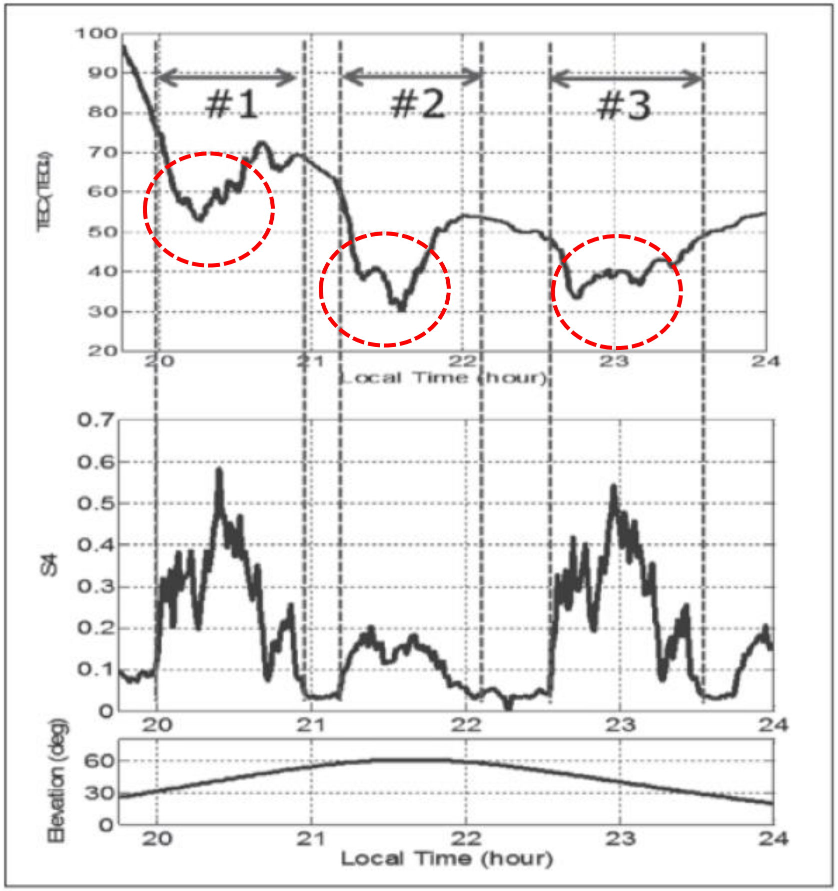

[Tsujii et al., Journal of the Korean Society of Surveying, Geodesy, Photogrammetry and Cartography, 2012]

Geometric Range vs. Pseudorange

Pseudorange: R(t)

$$R(t) = \rho^j + offset + noise$$

True Geometric range: ρ^j

$$\rho^j = \sqrt{\left(X^j - X_i\right)^2 + \left(Y^j - Y_i\right)^2 + \left(Z^j - Z_i\right)^2}$$

$$R(t) \neq \rho^j$$

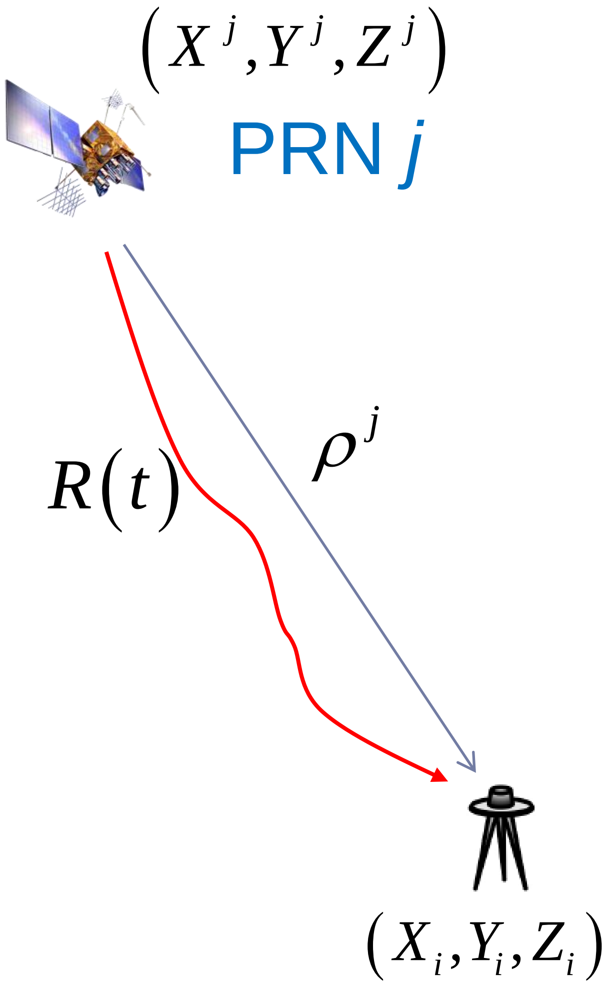

Pseudorange *R*

- The pseudorange $R(t)$ at time t (at the receiver)

$$R(t) = c\tau + c\left(b_s^j - b_r\right) + \varepsilon_{mult}(t) + n$$

$$R(t) = \underbrace{\rho(t, t-\tau)}_{1} + \underbrace{\delta_{ion}(t)}_{2} + \underbrace{\delta_{tro}(t)}_{3} + c\left(\underbrace{b_s^j}_{4} - \underbrace{b_r}_{5}\right) + \varepsilon_{mult}(t) + n$$

t = arrival time at the receiver

$t-\tau$ = emission time from the satellite

τ = transit time

δt_u = receiver clock bias

δt^s = satellite clock bias

$\varepsilon_{mult}(t)$ = multipath

n = errors

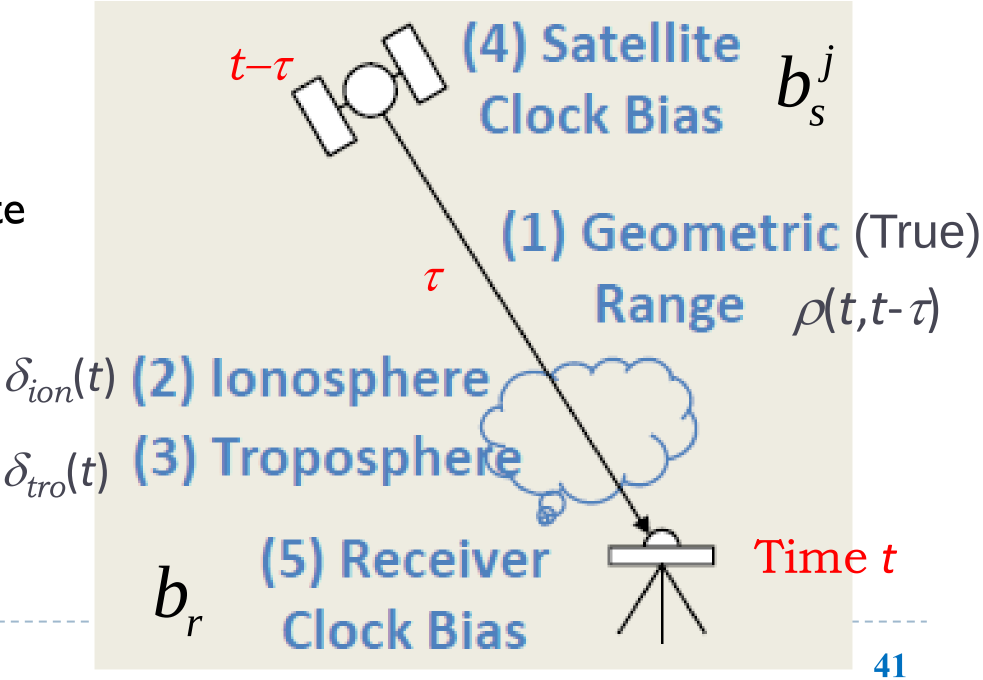

Klobuchar Model

8 Iono parameters in GPS navigation message

$$\alpha_0, \alpha_1, \alpha_2, \alpha_3, \quad \beta_0, \beta_1, \beta_2, \beta_3$$

cos(x)

$$T_{Iono} = \begin{cases} F \times 5\times10^{-9} & ;(|x| > 1.57) \\ F \times \left(5\times10^{-9} + \sum_{n=0}^{3} \alpha_n \phi_m^n \times \left(1 - \frac{x^2}{2} + \frac{x^4}{24}\right)\right) & ;(|x| \le 1.57) \end{cases}$$

Accuracy ~ 50-60%

Vertical iono delay

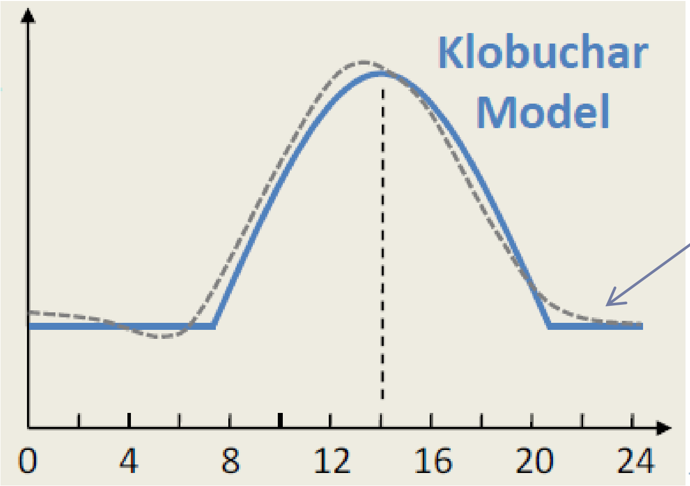

Local time

Fixed (nighttime)

- International GNSS Service
  - https://igs.org/

- Thailand
  - Royal Thai Survey Department – National Continuous Operating Reference Station (CORS) Network Portal
    - https://gnss-portal.rtsd.mi.th/portal/apps/sites/#/gnss
  - Land Department
  - Department of Public Works and Town Planning
  - GISTDA, Thai Meteorology Department, Hydro Informatics Institute)
  - KMITL, Chula (IGS), etc.

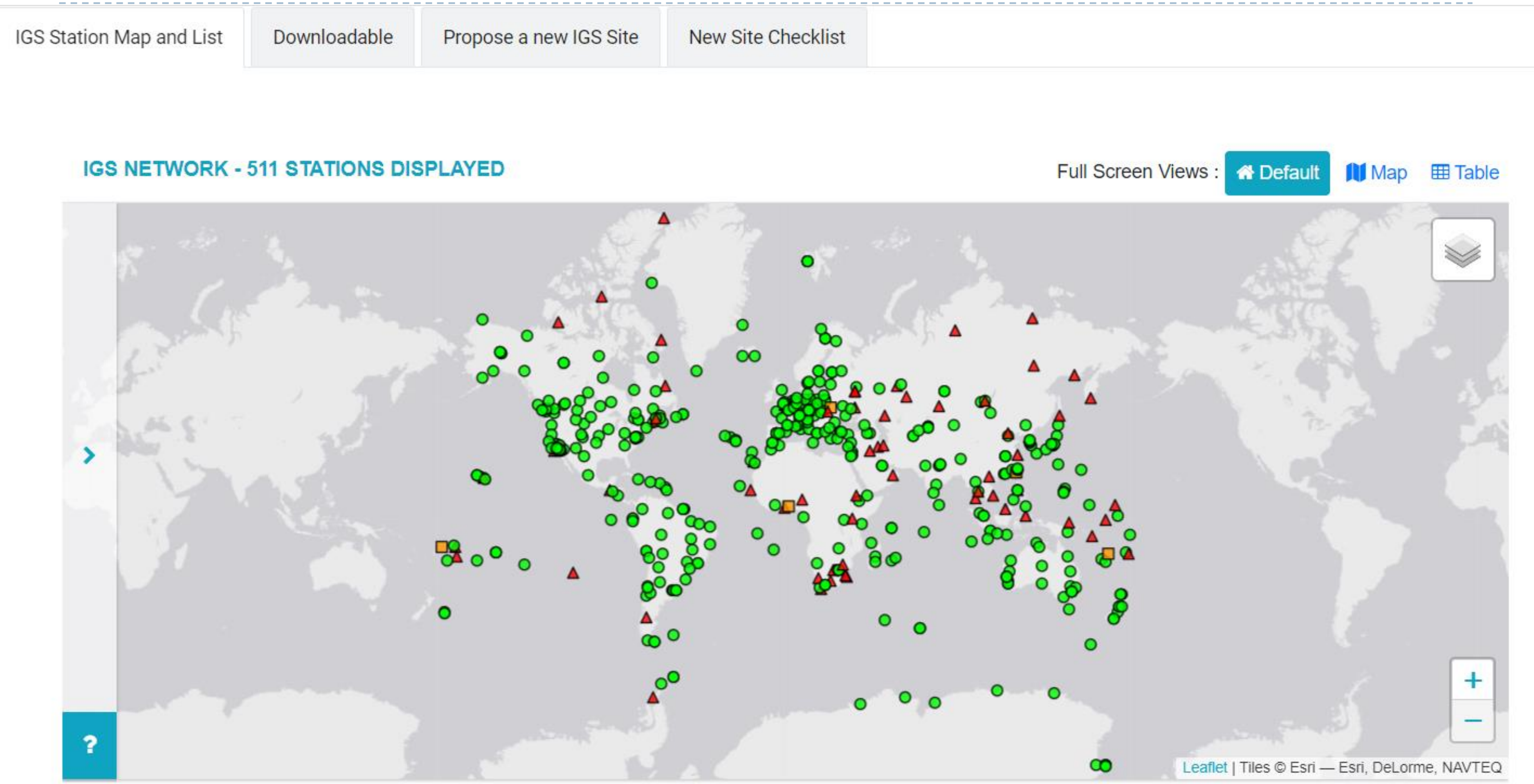

https://igs.org/network/#station-map-list

CORS stations in Thailand

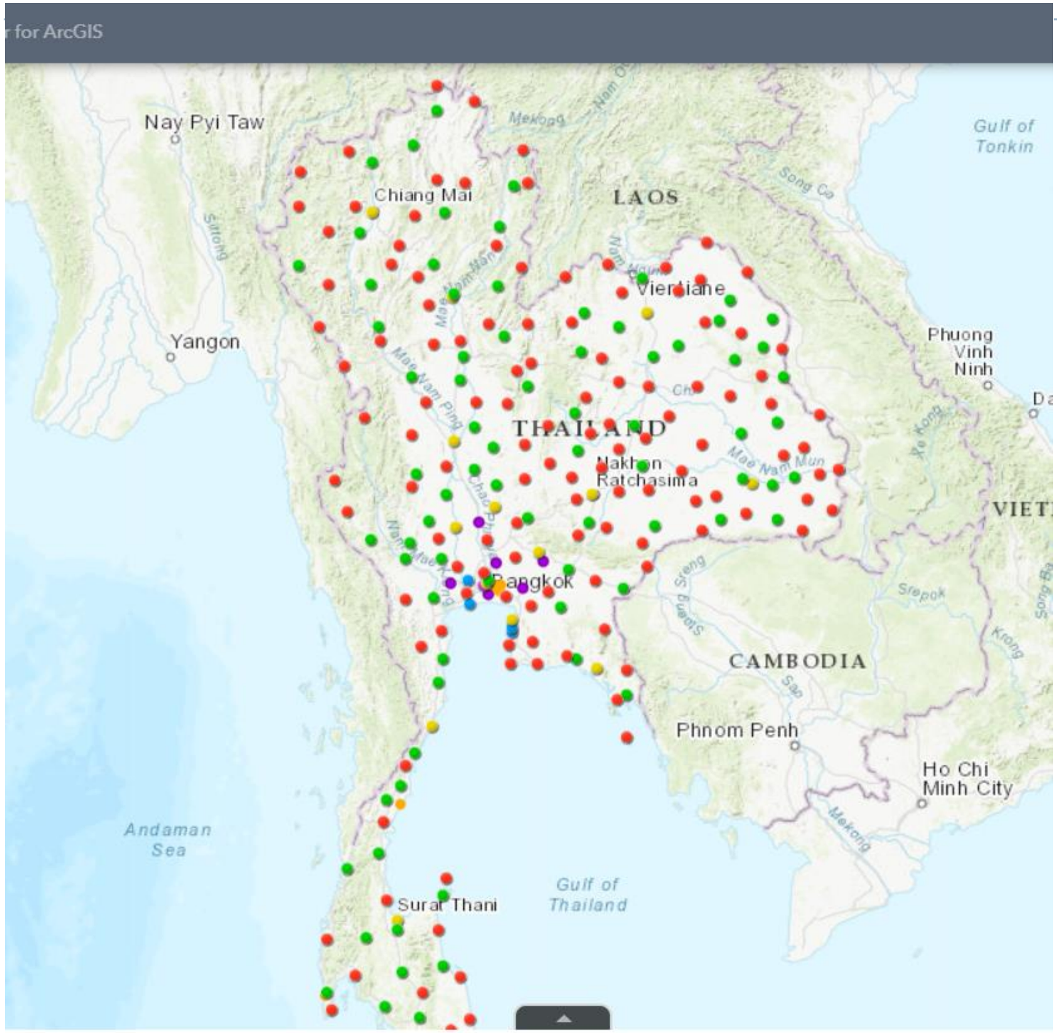

>200 stations

https://gnss-portal.rtsd.mi.th/portal/apps/sites/#/gnss/app/867489364d274483889292366dea9560